Article

# Mechanisms of C–C and C–H Alkane Reductive Eliminations from Octahedral Pt(IV): Reaction via Five-Coordinate Intermediates or Direct Elimination?

Dawn M. Crumpton-Bregel, and Karen I. Goldberg

*J. Am. Chem. Soc.*, **2003**, 125 (31), 9442-9456• DOI: 10.1021/ja029140u • Publication Date (Web): 11 July 2003



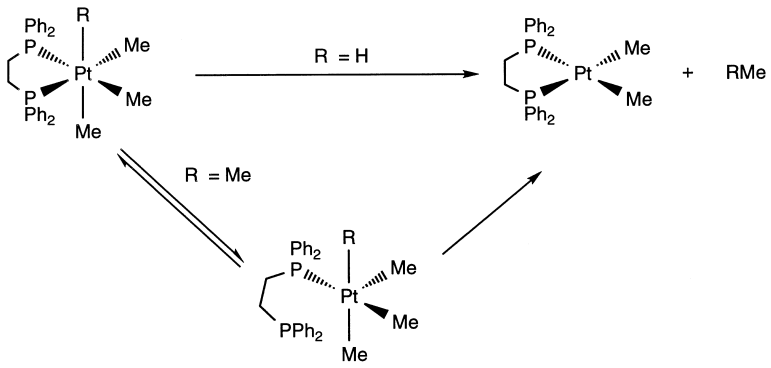


## More About This Article

Additional resources and features associated with this article are available within the HTML version:

- Supporting Information
- Links to the 17 articles that cite this article, as of the time of this article download
- Access to high resolution figures
- Links to articles and content related to this article
- Copyright permission to reproduce figures and/or text from this article

View the Full Text HTML

J|A|C|S
ARTICLES
Published on Web 07/11/2003

# Mechanisms of C−C and C−H Alkane Reductive Eliminations from Octahedral Pt(IV): Reaction via Five-Coordinate Intermediates or Direct Elimination?

Dawn M. Crumpton-Bregel and Karen I. Goldberg*

*Contribution from the Department of Chemistry, Box 351700, University of Washington, Seattle, Washington 98195-1700*

Received October 29, 2002; E-mail: goldberg@chem.washington.edu

***Abstract:*** The Pt(IV) complexes $P_2PtMe_3R$ [$P_2$ = dppe ($PPh_2(CH_2)_2PPh_2$), dppbz (*o*-$PPh_2(C_6H_4)PPh_2$); R = Me, H] undergo reductive elimination reactions to form carbon−carbon or carbon−hydrogen bonds. Mechanistic studies have been carried out for both C−C and C−H coupling reactions and the reductive elimination reactions to form ethane and methane are directly compared. For C−C reductive elimination, the evidence supports a mechanism of initial phosphine chelate opening followed by C−C coupling from the resulting five-coordinate intermediate. In contrast, mechanistic studies on C−H reductive elimination support an unusual pathway at Pt(IV) of *direct coupling without preliminary ligand loss*. The complexes *fac*-$P_2PtMe_3R$ ($P_2$ = dppe, R = Me, H; $P_2$ = dppbz, R = Me) have been characterized crystallographically. The Pt(IV) hydrides, *fac*-$P_2PtMe_3H$ ($P_2$ = dppe, dppbz), are rare examples of stable phosphine ligated Pt(IV) alkyl hydride complexes.

## Introduction

Reductive elimination to form a carbon−carbon or carbon−hydrogen bond is often the critical product release step in organic transformations mediated by transition-metal complexes.[1,2] The microscopic reverse, oxidative addition of a carbon−carbon or carbon−hydrogen bond serves as the substrate activation step in many stoichiometric and catalytic processes, including hydrocarbon functionalization.[1−5] The importance of these bond cleavage/formation processes in homogeneous catalysis has prompted numerous studies of the mechanisms of C−C and C−H oxidative addition and reductive elimination reactions.[1,3−6] Despite this large research effort, however, it remains difficult to predict the detailed mechanistic pathways of these reactions. Specifically, it is often unknown whether a particular reaction will proceed directly or will require ancillary ligand dissociation or even association prior to bond cleavage/formation.[1] Such explicit information concerning the reaction mechanism would be of enormous value to current efforts to rationally develop novel catalytic processes.

Many metal catalyzed reactions proceed via pathways involving oxidative addition to a $d^8$ square-planar metal center followed later in the cycle by reductive elimination from an

(1) (a) Collman, J. P.; Hegedus, L. S.; Norton, J. R.; Finke, R. G. *Principles and Applications of Organotransition Metal Chemistry*; University Science Books: Mill Valley, CA, 1987. (b) Atwood, J. D. *Inorganic and Organometallic Reaction Mechanisms*, 2nd ed. Wiley-VCH: New York, 1997. (c) Crabtree, R. H. *The Organometallic Chemistry of the Transition Metals*, 3rd ed.; John Wiley & Sons: New York, 2001. (d) Parshall, G. W.; Ittel, S. D. *Homogeneous Catalysis: The Applications and Chemistry of Catalysis by Soluble Transition Metal Complexes*, 2nd ed.; Wiley-Interscience: New York, 1992.

(2) (a) Cohen, R.; van der Boom, M. E.; Shimon, L. J. W.; Rozenberg, H.; Milstein, D. *J. Am. Chem. Soc*. **2000**, *122*, 7723. (b) Kakiuchi, F.; Murai, S. *Acc. Chem. Res*. **2002**, *35*, 826. (c) Sezen, B.; Franz, R.; Sames, D. *J. Am. Chem. Soc.* **2002**, *124*, 13 372.

(3) (a) Arndtsen, B. A.; Bergman, R. G.; Mobley, T. A.; Peterson, T. H. *Acc. Chem. Res*. **1995**, *28*, 154. (b) Shilov, A. E.; Shul′pin, G. B. *Chem. Rev.* **1997**, *97*, 2879. (c) Sen, A. *Acc. Chem. Res.* **1998**, *31*, 550. (d) Stahl, S. S.; Labinger, J. A.; Bercaw, J. E. *Angew. Chem., Int. Ed. Engl.* **1998**, *37*, 2181. (e) Shilov, A. E.; Shul'pin, G. B. *Activation and Catalytic Reactions of Saturated Hydrocarbons in the Presence of Metal Complexes*; Kluwer: Boston, 2000. (f) Crabtree, R. H. *J. Chem. Soc., Dalton Trans.* **2001**, 2437. (g) Labinger, J. A.; Bercaw, J. E. *Nature* **2002**, *417*, 507. (h) Fekl, U.; Goldberg, K. I. *Adv. Inorg. Chem.* **2003**, *54*, 259.

(4) (a) Jones, W. D. In *Topics in Organometallic Chemistry*; Murai, S., Ed.; Springer-Verlag: New York, 1999; Vol. 3, p 9. (b) Kakiuchi, F.; Murai, S. In *Topics in Organometallic Chemistry*; Murai, S., Ed.; Springer-Verlag: New York, 1999; Vol. 3, p 47. (c) Sen, A. In *Topics in Organometallic Chemistry*; Murai, S., Ed.; Springer-Verlag: New York, 1999; Vol. 3, p 81. (d) Murakami, M.; Ito, Y. In *Topics in Organometallic Chemistry*; Murai, S., Ed.; Springer-Verlag: New York, 1999; Vol. 3, p 97.

(5) (a) Rybtchinski, B.; Milstein, D. *Angew. Chem., Int. Ed. Engl*. **1999**, *38*, 870. (b) Perthuisot, C.; Edelbach, B. L.; Zubris, D. L.; Simhai, N.; Iverson, C. N.; Muller, C.; Satoh, T.; Jones, W. D. *J Mol. Catal. A Chem.* **2002**, *189*, 157.

(6) For some specific examples, see refs 7−28.

(7) (a) Brown, M. P.; Puddephatt, R. J.; Upton, C. E. E. *J. Chem. Soc., Dalton Trans*. **1974**, 2457. (b) Roy, S.; Puddephatt, R. J.; Scott, J. D. J. *J. Chem. Soc., Dalton Trans.* **1989**, 2121. (c) Goldberg, K. I.; Yan, J. Y.; Breitung, E. M. *J. Am. Chem. Soc.* **1995**, *117*, 6889. (d) Williams, B. S.; Holland, A. W.; Goldberg, K. I. *J. Am. Chem. Soc.* **1999**, *121*, 252. (e) Hill, G. S.; Yap, G. P. A.; Puddephatt, R. J. *Organometallics* **1999**, *18*, 1408. (f) Crumpton, D. M.; Goldberg, K. I. *J. Am. Chem. Soc*. **2000**, *122*, 962. (g) Williams, B. S.; Goldberg, K. I. *J. Am. Chem. Soc.* **2001**, *123*, 2576.

(8) (a) Byers, P. K.; Canty, A. J.; Crespo, M.; Puddephatt, R. J.; Scott, J. D. *Organometallics* **1988**, *7*, 1363. (b) Aye, K. T.; Canty, A. J.; Crespo, M.; Puddephatt, R. J.; Scott, J. D.; Watson, A. A. *Organometallics* **1989**, *8*, 2709. (c) Canty, A. J. *Acc. Chem. Res.* **1992**, *25*, 83 and references therein. (d) van Asselt, R.; Rijnberg, E.; Elsevier, C. J. *Organometallics* **1994**, *13*, 706. (e) Markies, B. A.; Canty, A. J.; Boersma, J.; van Koten, G. *Organometallics* **1994**, *13*, 2053. (f) Dücker-Benfer, C.; van Eldik, R.; Canty, A. J. *Organometallics* **1994**, *13*, 2412. (g) Canty, A. J. In *Comprehensive Organometallic Chemistry*, 2nd ed.; Puddephatt, R. J., Ed.; Pergamon: New York, 1995; Volume 9, Chapter 5 and references therein. (h) Kruis, D.; Markies, M. A.; Canty, A. J.; Boersma, J.; van Koten, G. *J Organomet. Chem*. **1997**, *532*, 235. (i) Canty, A. J.; Hoare, J. L.; Davies, N. W.; Traill, P. R. *Organometallics* **1998**, *17*, 2046. (j) Canty, A. J.; Hoare, J. L.; Patel, J.; Pfeffer, M.; Skelton, B. W.; White, A. H. *Organometallics* **1999**, *18*, 2660. (k) Bayler, A.; Canty, A. J.; Edwards, P. G.; Skelton, B. W.; White, A. H. *J. Chem. Soc., Dalton Trans*. **2000**, 3325, and references therein.

 **10.1021/ja029140u CCC: $25.00** 

octahedral $d^6$ center.[1] The mechanisms of oxidative addition reactions to $d^8$ metal centers and reductive elimination reactions from $d^6$ metal centers are thus of considerable interest. The formation of alkanes by C−C and C−H reductive elimination from $d^6$ octahedral complexes, in particular, has been extensively studied. Carbon−carbon coupling of two alkyl groups is frequently observed from Pt(IV) and Pd(IV) complexes,[7−9] but there are very few examples of this reaction from other $d^6$ metal centers.[10] Mechanistic investigations of $sp^3C$-$sp^3C$ reductive elimination reactions from octahedral Pt(IV) and Pd(IV) complexes have consistently found evidence for a five-coordinate intermediate from which the C−C bond formation takes place.[7,8,11,12] This five-coordinate intermediate is formed by ligand loss from the starting octahedral complex. The reactivity and stability of Pt(IV) and Pd(IV) alkyl complexes vary significantly with respect to the ancillary ligands present. For Pt(IV), C−C bond formation is common for complexes with phosphine ligands.[7] In contrast, complexes with Cp or nitrogen ligands are generally resistant to reductive elimination.[8d,13,14] A notable exception is the recent report of ethane reductive elimination from a nitrogen ligated five-coordinate Pt(IV) trimethyl complex.[9] For Pd(IV) alkyls, most phosphine ligated species appear to be too unstable to isolate or even observe.[8c,g,k] Instead, C−C reductive elimination from Pd(IV) has been commonly observed and studied from Pd(IV) alkyls complexes bearing nitrogen ligands.[8] Very little has been reported on alkyl C−C reductive elimination from late metal centers other than platinum or palladium. However, it should be noted that alkyl−alkyl coupling from an octahedral Rh(III) center was observed only when a five-coordinate intermediate was accessible.[10] Support for the involvement of five-coordinate intermediates in $sp^2C$-$sp^3C$ couplings from Ru(II) and Ir(III) has also been presented.[15] Thus, based on the limited empirical evidence, alkane C−C reductive elimination from $d^6$ octahedral complexes seems to require a five-coordinate intermediate.[11]

C−H reductive elimination reactions from $d^6$ octahedral metal centers do not, in general, follow as distinctive a pattern in terms of mechanism as C−C reductive elimination reactions. For alkyl and hydrocarbyl hydride complexes of the late metals Ir(III), Rh(III), Os(II), and Ru(II), some reactions are proposed to go by direct reductive elimination, whereas others require ligand dissociation prior to C−H coupling.[16−19] In contrast, all of the examples of C−H reductive elimination from Pt(IV) alkyl hydrides that have been studied to date were found to proceed via a preliminary ligand dissociation pathway.[3d,g,h,12,20−22] In fact, the recent discoveries of thermally stable Pt(IV) alkyl hydrides have been attributed to the use of chelating and other types of ligands which do not easily undergo dissociation to allow formation of five-coordinate species.[22,23] Of note, nearly all of the Pt(IV) hydrocarbyl hydrides reported contain nitrogen ancillary ligands.[24] Nitrogen ligands generally stabilize Pt(IV) and Pd(IV) to a greater extent than phosphine ligands.[8,14,25] However, even with nitrogen ligands, there are no examples of stable or even observable Pd(IV) alkyl hydrides. This has necessarily precluded any studies of C−H reductive elimination from Pd(IV). Overall, it seems that the mechanisms as well as the thermodynamics of C−H reductive elimination are quite sensitive to the identities of the metal and the ligand set. Further studies are clearly required to gain general predictive power concerning these reactions.

Although C−C and C−H reductive elimination of alkanes is known to occur from several different late metals, Pt(IV) shows the most examples of both reactions, and is therefore the most promising for use in a study to directly compare the mechanisms of C−C and C−H coupling. As noted above, in virtually every investigation of *either* C−C or C−H reductive elimination of alkanes from octahedral Pt(IV) complexes,

(9) (a) Fekl, U.; Kaminsky, W.; Goldberg, K. I. *J. Am. Chem. Soc.* **2001**, *123*, 6423. (b) Fekl, U.; Goldberg, K. I. *J. Am. Chem. Soc.* **2002**, *124*, 6804.
(10) Hahn, C.; Spiegler, M.; Herdtweck, E.; Taube, R. *Eur. J. Inorg. Chem.* **1999**, 435.
(11) A possible exception: a kinetic fit analysis indicated that in the absence of added L, 1−2% of thermally promoted C−C reductive elimination from $L_2PtMe_4$ (L = MeNC, 2,6-$Me_2C_6H_3NC$) proceeds without ligand dissociation. However, significant decomposition of L under the reaction conditions hindered a complete analysis of the data.[7b]
(12) Puddephatt, R. J. *Angew. Chem., Int. Ed. Engl.* **2002**, *41*, 261.
(13) (a) Egger, K. W. *J. Organomet. Chem.* **1970**, *24*, 501. (b) Gschwind, R. M.; Schlecht, S. *J. Chem. Soc., Dalton Trans.* **1999**, 1891.
(14) Rendina, L. M.; Puddephatt, R. J. *Chem Rev.* **1997**, *97*, 1735.
(15) (a) Saunders, D. R.; Mawby, R. J. *J. Chem. Soc., Dalton Trans.* **1984**, 2133. (b) Thompson, J. S.; Atwood, J. D. *Organometallics* **1991**, *10*, 3525.
(16) (a) Basato, M.; Longato, B.; Morandini, F.; Bresadola, S. *Inorg. Chem.* **1984**, *23*, 3972. (b) Buchanan, J. M.; Stryker, J. M.; Bergman, R. G. *J. Am. Chem. Soc.* **1986**, *108*, 1537. (c) Deutsch, P. P.; Eisenberg, R. *J. Am. Chem. Soc.* **1990**, *112*, 714. (d) Harper, T. G. P.; Desrosiers, P. J.; Flood, T. C. *Organometallics* **1990**, *9*, 2523. (e) Thompson, J. S.; Bernard, K. A.; Rappoli, B. J.; Atwood, J. D. *Organometallics* **1990**, *9*, 2727. (f) Cleary, B. P.; Mehta, R.; Eisenberg, R. *Organometallics* **1995**, *14*, 2297. (g) Aizenberg, M.; Milstein, D. *J. Am. Chem. Soc.* **1995**, *117*, 6456. (h) Okazaki, M.; Tobita, H.; Kawano, Y.; Inomata, S.; Ogino, H. *J. Organomet. Chem.* **1998**, *553*, 1. (i) Rosini, G. P.; Wang, K.; Patel, B.; Goldman, A. S. *Inorg. Chimica. Acta* **1998**, *270*, 537. (j) Wiley, J. S.; Oldham, W. J.; Heinekey, D. M. *Organometallics* **2000**, *19*, 1670. (k) Kanzelberger, M.; Singh, B.; Czerw, M.; Krogh-Jespersen, K.; Goldman, A. S. *J. Am. Chem. Soc.* **2000**, *122*, 11 017.
(17) (a) Milstein, D. *J. Am. Chem. Soc.* **1982**, *104*, 5227. (b) Milstein, D. *Acc. Chem. Res.* **1984**, *17*, 221. (c) Jones, W. D.; Feher, F. J. *J. Am. Chem. Soc.* **1984**, *106*, 1650. (d) Periana, R. A.; Bergman, R. G. *J. Am. Chem. Soc.* **1986**, *108*, 7332. (e) Jones, W. D.; Feher, F. J. *Acc. Chem. Res.* **1989**, *22*, 91. (f) Selmeczy, A. D.; Jones, W. D.; Osman, R.; Perutz, R. N. *Organometallics* **1995**, *14*, 4677. (g) Wick, D. D.; Reynolds, K. A.; Jones, W. D. *J. Am. Chem. Soc.* **1999**, *121*, 3974. (h) Northcutt, T. P.; Wick, D. D.; Vetter, A. J.; Jones, W. D. *J. Am. Chem. Soc.* **2001**, *123*, 7257. (i) Jones, W. D. *Acc. Chem. Res.* **2003**, *36*, 140.
(18) Shinomoto, R. S.; Desrosiers, P. J.; Harper, T. G. P.; Flood, T. C. *J. Am. Chem. Soc.* **1990**, *112*, 704.
(19) (a) Hartwig, J. F.; Andersen, R. A.; Bergman, R. G. *J. Am. Chem. Soc.* **1991**, *113*, 6492. (b) Hartwig, J. F.; Andersen, R. A.; Bergman, R. G. *Organometallics* **1991**, *10*, 1710. (c) Hsu, G. C.; Kosar, W. P.; Jones, W. D. *Organometallics* **1994**, *13*, 385.
(20) (a) Stahl, S. S.; Labinger, J. A.; Bercaw, J. E. *J. Am. Chem. Soc.* **1996**, *118*, 5961. (b) Jenkins, H. A.; Yap, G. P. A.; Puddephatt, R. J. *Organometallics* **1997**, *16*, 1946. (c) Fekl, U.; Zahl, A.; van Eldik, R. *Organometallics* **1999**, *18*, 4156. (d) Reinartz, S.; White, P. S.; Brookhart, M.; Templeton, J. L. *Organometallics* **2000**, *19*, 3854. (e) Reinartz, S.; White, P. S.; Brookhart, M.; Templeton, J. L. *Organometallics* **2001**, *20*, 1709. (f) Reinartz, S.; Baik, M.-H.; White, P. S.; Brookhart, M.; Templeton, J. L. *Inorg. Chem.* **2001**, *40*, 4726. (g) Reinartz, S.; White, P. S.; Brookhart, M.; Templeton, J. L. *J. Am. Chem. Soc.* **2001**, *123*, 12724. (h) Norris, C. M.; Reinartz, S.; White, P. S.; Templeton, J. L. *Organometallics* **2002**, *21*, 5649. (i) Prokopchuk, E. M.; Puddephatt, R. J. *Organometallics* **2003**, *22*, 563. (j) Prokopchuk, E. M.; Puddephatt, R. J. *Organometallics* **2003**, *22*, 787. (k) Jensen, M. P.; Wick, D. D.; Reinartz, S.; White, P. S.; Templeton, J. L.; Goldberg, K. I. *J. Am. Chem. Soc.* **2003**, published ASAP on the Web June 18, 2003.
(21) (a) Hill, G. S.; Rendina, L. M.; Puddephatt, R. J. *Organometallics* **1995**, *14*, 4966. (b) Jenkins, H. A.; Yap, G. P. A.; Puddephatt, R. J. *Organometallics* **1997**, *16*, 1946. (c) Hinman, J. G.; Baar, C. R.; Jennings, M. C.; Puddephatt, R. J. *Organometallics* **2000**, *19*, 563. (d) Johansson, L.; Tilset, M. *J. Am. Chem. Soc.* **2001**, *123*, 739. (e) Wik, B. J.; Lersch, M.; Tilset, M. *J. Am. Chem. Soc.* **2002**, *124*, 12 116.
(22) A recent review of Pt(IV) hydrides does suggest that direct C−H reductive elimination may be possible. Puddephatt, R. J. *Coord. Chem. Rev.* **2001**, *219*, 157.
(23) (a) O'Reilly, S.; White, P. S.; Templeton, J. L. *J. Am. Chem. Soc.* **1996**, *118*, 5684. (b) Canty, A. J.; Dedieu, A.; Jin, H.; Milet, A.; Richmond, M. K. *Organometallics* **1996**, *15*, 2845. (c) Hill, G. S.; Vittal, J. J.; Puddephatt, R. J. *Organometallics* **1997**, *16*, 1209. (d) Prokopchuk, E. M.; Jenkins, H. A.; Puddephatt, R. J. *Organometallics* **1999**, *18*, 2861. (e) Haskel, A.; Keinan, E. *Organometallics* **1999**, *18*, 4677. (f) Reinartz, S.; Brookhart, M.; Templeton, J. L. *Organometallics* **2002**, *21*, 247. (g) Iron, M. A.; Lo, H. C.; Martin, J. M. L.; Keinan, E. *J. Am. Chem. Soc.* **2002**, *124*, 7041.
(24) The only previously reported example of a Pt(IV) alkyl hydride complex with phosphine ligands is $(PEt_3)_2Pt(CH_3)_2(H)Cl$.[20a] This complex undergoes reductive elimination of methane, but mechanistic details were not reported.
(25) Hill, G. S.; Puddephatt, R. J. *Organometallics* **1998**, *17*, 1478.

mechanistic evidence supports a reaction pathway of ancillary ligand dissociation to form a five-coordinate intermediate prior to reductive elimination.[7,12,20,21] There have been no unambiguous examples of direct alkyl−alkyl or alkyl−hydride coupling from an octahedral Pt(IV) complex.[11] This has led to a general belief that such eliminations from Pt(IV) *require* a five-coordinate intermediate.[22] This proposal has been further supported by the observation that Pt(II) centers which undergo facile intermolecular activation of C−H bonds all share in common the presence of a labile ligand or an alternative means of generating a site at Pt(II) to which the hydrocarbon can coordinate.[9b,20e,h,k,26,27] This apparent "requirement" for C−H oxidative addition to Pt(II) would be consistent, by the principle of microscopic reversibility, with the preliminary ligand dissociation observed for C−H reductive elimination from Pt(IV). The oxidative addition of C−H bonds to Pt(II) is currently of great interest as such reactivity is proposed as the key substrate activation step in platinum-catalyzed selective alkane oxidation reactions, so-called Shilov chemistry.[3] It should also be noted that C−C activation at Pt(II) has only been reported to occur at unsaturated Pt(II) centers.[28]

Is this large pool of empirical evidence concerning preliminary ligand dissociation meaningful as a predictor of the mechanism of C−H and C−C reductive eliminations from Pt(IV) and oxidative additions to Pt(II), or is it merely a consequence of the particular Pt(IV) complexes chosen for study? In this contribution, we address this question by reporting the first examples of isolable Pt(IV) alkyl hydrides bearing phosphine ligands and mechanistic investigations of C−H reductive elimination of methane from these complexes. Evidence is presented for the first alkane reductive elimination reaction from Pt(IV) that proceeds directly without ligand dissociation. In addition, detailed mechanistic investigations of C−C reductive elimination from the complementary Pt(IV) alkyl complexes to produce ethane are also reported.[29] Thus, Me−Me and Me−H reductive elimination reactions from the same metal center can be directly compared for the first time. Because both C−C and C−H reductive elimination reactions proceed via similar concerted three-center transition states involving cis $\sigma$-only donor ligands on the metal center,[1] these couplings have often been used to model one another. However, because the propensities for these two types of reactions differ so dramatically, direct comparison of the couplings in the same metal ligand environment has been challenging. If alkyl C−H reductive elimination is observable, then alkyl C−C coupling appears to require a sufficiently high temperature such that competing decomposition reactions ensue. Similarly, if alkyl C−C coupling is observable, the corresponding metal alkyl hydride is too reactive to detect even at much lower temperatures. Thermolyses of the phosphine ligated Pt(IV) complexes $L_2PtMe_3R$ ($L_2$ = dppe ($PPh_2(CH_2)_2PPh_2$), dppbz (*o*-$PPh_2(C_6H_4)PPh_2$); R = Me, H) has allowed for a direct comparison of the mechanisms of these coupling reactions: C−C reductive elimination takes place from a five-coordinate intermediate, whereas the more facile C−H elimination proceeds directly from the octahedral geometry.

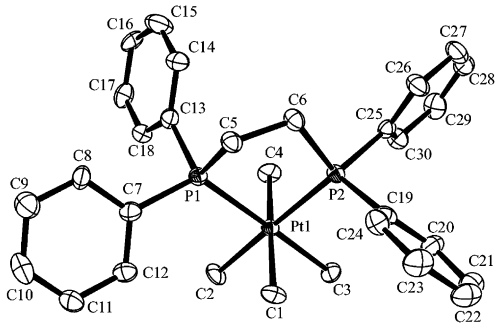


***Figure 1.*** ORTEP diagram for (dppe)$PtMe_4$ (**1**), with hydrogen atoms omitted for clarity.

## Results

**Synthesis and Characterization of $L_2PtMe_3R$ ($L_2$ = dppe, dppbz; R = Me, Et or H).** The tetraalkyl complexes (dppe)-$PtMe_4$ (**1**),[30] (dppbz)$PtMe_4$ (**2**), and (dppe)$PtMe_3Et$ (**3**) were prepared by addition of an alkyllithium or alkyl Grignard reagent to the corresponding $L_2PtMe_3I$ ($L_2$ = dppe, dppbz) complex. The isotopically labeled analogues of **1**, *fac*-dppePtMe$(CD_3)_3$ (***fac*-1-*d*$_9$**) and dppe$Pt(CD_3)_4$ (**1-*d*$_{12}$**), were prepared by similar methods using deuterated methylating reagents.

The trimethylhydride complexes *fac*-(dppe)$PtMe_3H$ (**4**) and *fac*-(dppbz)$PtMe_3H$ (**5**) were prepared by addition of a sodium borohydride reagent ($NaBH_4$ or $NaBH_3CN$) to the trimethyl acetate derivative $L_2PtMe_3(OAc)$ ($L_2$ = dppe, dppbz).[7g] The deuterated analogues of **4** and **5**, *fac*-(dppe)$PtMe_3D$ (**4-*d*$_1$**) and *fac*-(dppbz)$PtMe_3D$ (**5-*d*$_1$**) were prepared using borodeuteride reagents. Significant amounts of the Pt(II) complexes, $L_2PtMe_2$ formed during the preparation of the Pt(IV) trimethylhydride complexes and even after multiple recrystallizations, small amounts of $L_2PtMe_2$ (9−21%) remained in the isolated samples of **4**, **4-*d*$_1$**, **5**, and **5-*d*$_1$**. This was the only Pt impurity detected, and it was determined that the presence of $L_2PtMe_2$ did not affect the studies of methane reductive elimination from these complexes (see below).

The complexes **1**, **2**, and **4** were characterized by X-ray crystallography. The ORTEP diagrams are shown in Figures 1, 2, and 3. Table 1 contains the crystallographic data, and selected bond lengths and angles are listed in Tables 2 and 3. In each complex, the geometry deviates only slightly from octahedral, as indicated by the bond angles around Pt (84°−95°). The Pt−Me bond lengths vary only slightly with respect to the trans ligand. For Pt−Me trans to phosphorus, the average Pt−C bond length is 2.11 ± 0.01 Å (complexes **1**, **2**, and **4**). The Pt−C

(26) (a) Brainard, R. L.; Nutt, W. R.; Lee, T. R.; Whitesides, G. M. *Organometallics* **1988**, *7*, 2379. (b) Holtcamp, M. W.; Labinger, J. A.; Bercaw, J. E. *J. Am. Chem. Soc.* **1997**, *119*, 848. (c) Wick, D. D.; Goldberg, K. I. *J. Am. Chem. Soc.* **1997**, *119*, 10235. (d) Holtcamp, M. W.; Henling, L. M.; Day, M. W.; Labinger, J. A.; Bercaw, J. E. *Inorg. Chim. Acta* **1998**, *270*, 467. (e) Johansson, L.; Ryan, O. B.; Tilset, M. J. *J. Am. Chem. Soc.* **1999**, *121*, 1974. (f) Heiberg, H.; Johansson, L.; Gropen, O.; Ryan, O. B.; Swang, O.; Tilset, M. *J. Am. Chem. Soc.* **2000**, *122*, 10831. (g) Johansson, L.; Tilset, M.; Labinger, J. A.; Bercaw, J. E. *J. Am. Chem. Soc.* **2000**, *122*, 10 846. (h) Thomas, J. C.; Peters, J. C. *J. Am. Chem. Soc.* **2001**, *123*, 5100. (i) Johansson, L.; Ryan, O. B.; Rømming, C.; Tilset, M. *J. Am. Chem. Soc.* **2001**, *123*, 6579. (j) Harkins, S. B.; Peters, J. C. *Organometallics* **2002**, *21*, 1753. (k) Zhong, H. A.; Labinger, J. A.; Bercaw, J. E. *J. Am. Chem. Soc.* **2002**, *124*, 1378. (l) Konze, W. V.; Scott, B. L.; Kubas, G. J. *J. Am. Chem. Soc.* **2002**, *124*, 12550.

(27) (a) Vedernikov, A. N.; Caulton, K. G. *Angew Chem. Int Ed. Engl.* **2002**, *41*, 4102. (b) Vedernikov, A. N.; Caulton, K. G. *Chem. Commun.* **2003**, 358. (c) Vedernikov, A. N.; Huffman, J. C.; Caulton, K. G. *New J. Chem.* **2003**, *27*, 665.

(28) (a) van der Boom, M. E.; Kratz, H.-B.; Hassner, L.; Ben-David, Y.; Milstein, D. *Organometallics* **1999**, *18*, 3873. (b) Edelbach, B. L.; Lachicotte, R. J.; Jones, W. D. *J. Am. Chem. Soc.* **1998**, *120*, 2843.

(29) For a preliminary report, see ref 7f.

(30) (dppe)$PtMe_4$ was previously prepared by addition of dppe to $Pt_2(\mu\text{-}SMe_2)_2Me_8$. Lashanizadehgan, M.; Rashidi, M.; Hux, J. E.; Puddephatt, R. J. *J. Organomet. Chem.* **1984**, *269*, 317.

***Table 1.*** X-ray Diffraction Data for $P_2PtMe_3R$ Complexes

| | (dppe)$PtMe_4$ (**1**) | (dppbz)$PtMe_4$ (**2**) | (dppe)$PtMe_3H$ (**4**) |
|---|---|---|---|
| empirical formula | $C_{30}H_{36}P_2Pt$ | $C_{34}H_{36}P_2Pt$ | $C_{29}H_{34}P_2Pt$ |
| FW | 653.62 | 701.66 | 639.6 |
| $T$ (K) | 161(2) | 293 (2) | 161 |
| wavelength (Å) | 0.71070 | 0.71070 | 0.71070 |
| crystal description | colorless cube | colorless plate | colorless plate |
| crystal system, space group | orthorhombic, $Pna2_1$ | triclinic, $P_1$ | monoclinic, $P2_1/n$ (No. 14) |
| unit cell dimensions (Å, deg) | $a = 14.6533$ (2) | $a = 10.0224$ (4) | $a = 10.05560$ (10) |
| | $b = 11.7535$ (2) | $b = 11.1025$ (4) | $b = 17.0058$ (3) |
| | $c = 15.4973$ (1) | $c = 14.4028$ (6) | $c = 16.1268$ (3) |
| | $\alpha = 90$ | $\alpha = 83.390$ (2) | $\alpha = 90$ |
| | $\beta = 90$ | $\beta = 71.766$ (2) | $\beta = 107.0455$ (10) |
| | $\gamma = 90$ | $\gamma = 80.506$ (2) | $\gamma = 90$ |
| volume (Å$^3$) | 2669.06 (6) | 1497.88 (10) | 2636.60 (7) |
| $Z$, density (g/cm$^3$) | 4, 1.627 | 2, 1.556 | 4, 1.611 |
| absorption coefficient (mm$^{-1}$) | 5.393 | 4.811 | 5.458 |
| $F$ (000) | 1296 | 696 | 1264 |
| crystal size (mm) | 0.31 × 0.29 × 0.23 | 0.35 × 0.25 × 0.18 | 0.13 × 0.10 × 0.08 |
| reflection for indexing | 1726 | 46 | 1077 |
| $\theta$ range (deg) | 3.08 to 28.66 | 2.99 to 23.33 | 2.40 to 30.52 |
| index ranges | $-17 \le h \ge 17$ | $-11 \le h \ge 11$ | $-13 \le h \ge 13$ |
| | $-14 \le k \ge 14$ | $-12 \le k \ge 12$ | $-24 \le k \ge 24$ |
| | $-17 \le l \ge 16$ | $-15 \le l \ge 16$ | $-23 \le l \ge 23$ |
| reflections collected/ unique | 36929, 5191 | 15983, 4087 | 108784, 7550 |
| completeness to $2\theta$ | 81.9% | 94.1% | 90.7% |
| absorption correction | SORTAV | SORTAV | scalepack |
| refinement method | full-matrix least squares on $F^2$ | full-matrix least squares on $F^2$ | full-matrix least squares on $F^2$ |
| $R_{int}$ | 0.047 | 0.0826 | 0.0222 |
| parameters refined | 298 | 334 | 292 |
| goodness of fit on $F^2$ | 1.028 | 1.041 | 1.028 |
| final $R$, $R_w$ ($I > 2\sigma I$)[a] | 0.0302, 0.0949 | 0.0380, 0.0900 | 0.0352, 0.0824 |

[a] $w = 1/[\sigma^2(Fo^2) + (aP)^2 + bP]$; $P = (Fo^2 + 2Fc^2)/3$; $a = 0.0418$ for **1**, 0.0577 for **2** and 0.0316 for **4**; $b = 0.9579$ for **1**, 7.5138 for **2** and 6.9896 for **4**.

***Table 2.*** Selected Bond Lengths and Angles for $L_2PtMe_4$ Complexes

| | (dppe)$PtMe_4$ (**1**) | (dppbz)$PtMe_4$ (**2**) |
|---|---|---|
| | bond lengths (Å) | |
| $Pt-C_1$ | 2.139(7) | 2.151(8) |
| $Pt-C_4$ | 2.111(6) | 2.131(8) |
| $Pt-C_2$ | 2.115(6) | 2.108(7) |
| $Pt-C_3$ | 2.105(6) | 2.122(8) |
| $Pt-P_1$ | 2.3359(17) | 2.3275(15) |
| $Pt-P_2$ | 2.3250(16) | 2.3246(15) |
| | bond angles (deg) | |
| $P_1-Pt-P_2$ | 85.94(5) | 84.17(5) |
| $C_2-Pt-C_3$ | 84.0(3) | 87.3(4) |
| $C_1-Pt-C_4$ | 174.6(3) | 174.1(3) |
| $C_2-Pt-P_1$ | 95.4(2) | 93.9(3) |
| $C_3-Pt-P_2$ | 94.67(18) | 94.4(2) |

***Table 3.*** Selected Bond Lengths and Angles for *Fac*-(dppe)$PtMe_3H$ (**4**)

| bond lengths (Å) | | bond angles (deg) | |
|---|---|---|---|
| $Pt-H$ | 1.70(4) | $P_1-Pt-P_2$ | 86.04(3) |
| $Pt-C_1$ | 2.145(4) | $C_2-Pt-C_3$ | 87.44(17) |
| $Pt-C_2$ | 2.110(4) | $C_2-Pt-P_2$ | 92.93(11) |
| $Pt-C_3$ | 2.114(4) | $C_3-Pt-P_1$ | 93.54(13) |
| $Pt-P_1$ | 2.3141(10) | $H-Pt-C_1$ | 174.0(14) |
| $Pt-P_2$ | 2.3185(9) | | |

bond trans to methyl has an average length of 2.13 ± 0.02 Å (complexes **1** and **2**). With hydride as the trans ligand, the Pt–Me bond is 2.145(4) Å (complex **4**). The hydride in **4** was located and refined, and the Pt–H bond length was determined to be 1.70(4) Å.

***Scheme 1***

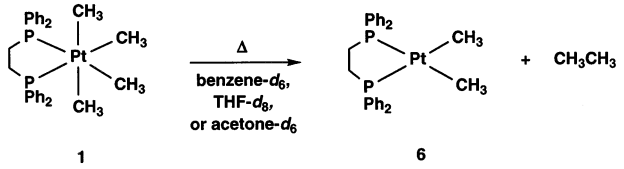


**1** **6**

**Thermolysis of $L_2PtMe_4$ ($L_2$ = dppe (1), dppbz (2)).** Thermolysis of (dppe)$PtMe_4$ (**1**) in solution at temperatures in excess of 150 °C yielded ethane and (dppe)$PtMe_2$[31] (**6**) in quantitative yield (Scheme 1). The reaction exhibited clean first-order kinetic behavior in benzene-$d_6$ ($k = 4.2 \pm 0.1 \times 10^{-6}$ s$^{-1}$), THF-$d_8$ ($k = 3.2 \pm 0.1 \times 10^{-6}$ s$^{-1}$) and acetone-$d_6$ ($k = 4.9 \pm 1.0 \times 10^{-6}$ s$^{-1}$).[32] Activation parameters of $\Delta H^{\ddagger} = 43 \pm 2$ kcal/mol and $\Delta S^{\ddagger} = 15 \pm 4$ eu were calculated from rate constants measured in benzene-$d_6$ over a temperature range of 165–205 °C. The Eyring plot is shown in Figure 4.

**Crossover Study.** A crossover study was performed in which an equimolar mixture of (dppe)$PtMe_4$ (**1**) and (dppe)$Pt(CD_3)_4$ (**1-*d*$_{12}$**) was heated in benzene-$d_6$ at 165 °C for slightly more than one half-life (50 h). Analysis by mass spectrometry showed that the gaseous products produced consisted of approximately equal amounts of $CH_3CH_3$ and $CD_3CD_3$, with less than 4% $CH_3$-$CD_3$. The Pt starting complexes and products were analyzed by $^{31}P$ NMR spectroscopy.[33] Prior to thermolysis, only signals

(31) Appleton, T. G.; Bennett, M. A.; Tomkins, I. B. *J. Chem. Soc., Dalton Trans.* **1976**, 439.
(32) See Supporting Information for kinetic plots.
(33) Attempts to characterize the Pt species present (both before and after thermolysis) by mass spectrometry were unsuccessful. Molecular ions were not detected using either direct insertion or electrospray techniques.

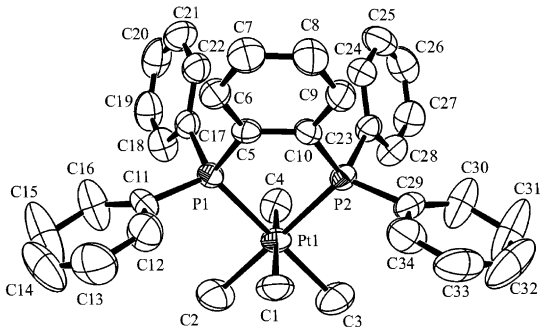


***Figure 2.*** ORTEP diagram for (dppbz)$PtMe_4$ (**2**), with hydrogen atoms omitted for clarity.

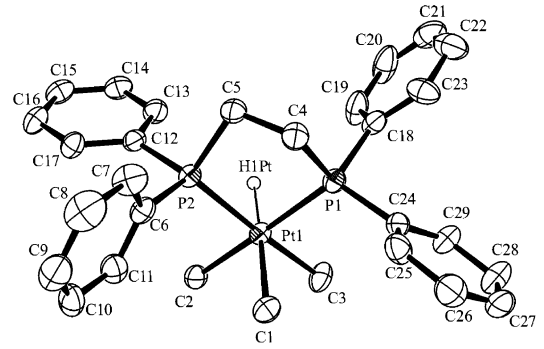


***Figure 3.*** ORTEP diagram for *fac*-(dppe)$PtMe_3H$ (**4**), with hydrogen atoms omitted for clarity.

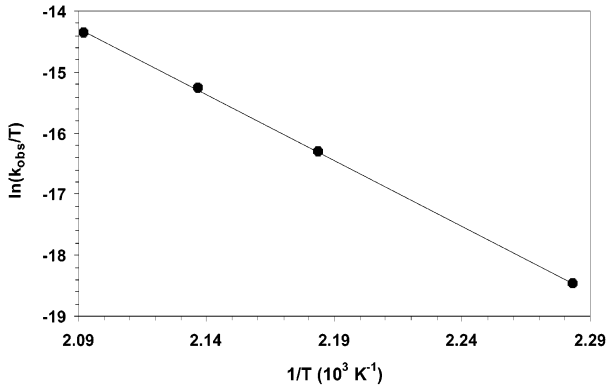


***Figure 4.*** Eyring plot for ethane elimination from **1** (165 to 205 °C) in benzene-$d_6$.

corresponding to **1** ($\delta$ 7.3, $J_{Pt-P}$ = 1145 Hz) and **1-$d_{12}$** ($\delta$ 7.4, $J_{Pt-P}$ = 1145 Hz) were observed in the $^{31}P$ NMR spectrum. After 50 h of thermolysis, these same two Pt(IV) phosphine signals were observed and there was no evidence of deuterium scrambling in the unreacted Pt(IV) species. However, $^{31}P$ NMR signals for three Pt(II) products, (dppe)$PtMe_2$ (**6**, $\delta$ 47.35, $J_{Pt-P}$ = 1779 Hz), (dppe)$PtMe(CD_3)$ (**6-$d_3$**, $\delta$ 47.42, $J_{Pt-P}$ = 1774 Hz), and (dppe)$Pt(CD_3)_2$ (**6-$d_6$**, $\delta$ 47.49, $J_{Pt-P}$ = 1769 Hz) were observed.[34] Unfortunately, these dppePt(II) signals were not baseline separated and integration was not possible, even at high field (202.5 MHz). To confirm that the deuterium scrambling among these Pt(II) complexes occurred after reductive elimination, an equimolar mixture of **6** and **6-$d_6$** in benzene-$d_6$ was heated at 165 °C for 12 h. $^{31}P$ NMR revealed the generation of a significant amount of **6-$d_3$**. The exchange of alkyl groups

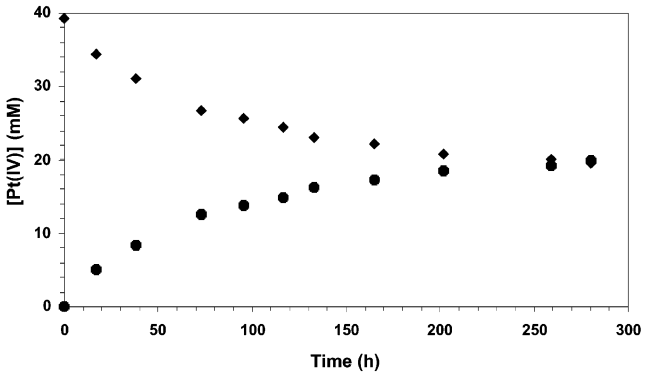


***Figure 5.*** Equilibrium plot of ***fac*-1-$d_9$** (♦) and ***mer*-1-$d_9$** (●) at 100 °C in benzene-$d_6$.

among $d^8$ M(II) (M = Pt, Pd) complexes at elevated temperatures has been reported by others.[35]

**Intramolecular Isomerization of *fac*-1-$d_9$.** Although the crossover experiment described above clearly showed that intermolecular exchange of methyl groups at Pt(IV) does not occur, intramolecular exchange of the methyl groups at Pt(IV) does take place. This was observed directly when the partially deuterated complex *fac*-(dppe)$PtMe(CD_3)_3$ (***fac*-1-$d_9$**) was heated at 100 °C in benzene-$d_6$. Slow isomerization of ***fac*-1-$d_9$** to a 1:1 mixture of ***fac*-1-$d_9$** and ***mer*-1-$d_9$** ($K_{eq}$ = 1) occurred (Figure 5). The progress of the reaction was conveniently monitored by $^1H$ NMR. The rate constant for the isomerization of ***fac*-1-$d_9$** to ***mer*-1-$d_9$** at 100 °C in benzene-$d_6$ was $k_f = 1.7 \times 10^{-6}$ $s^{-1}$.[32,36]

**Thermolysis of (dppbz)$PtMe_4$ (2).** The thermal behavior of (dppbz)$PtMe_4$ (**2**) was also examined. Similar to the dppe complex **1**, the solution thermolysis of **2** in THF-$d_8$ at 165 °C resulted in ethane elimination and the formation of the corresponding Pt(II) dimethyl complex, (dppbz)$PtMe_2$ (**7**). Reductive elimination from **2** was significantly slower than from **1** and in addition, the rate was not first-order in **2**. The rate of the reaction slowed considerably with time. In the first 100 h, 9−17% conversion was observed, yet between 100 and 500 h, only 5−13% additional conversion was detected. The amount of conversion measured varied within these ranges for each individual sample.

A trace amount of an impurity was suspected to be the cause of the fast initial rate. Although **2** was repeatedly purified by recrystallization, thermolysis reactions of **2** continued to decelerate with time. However, when the thermolyses of **2** were carried out in the presence of 2% cross-linked polyvinylpyridine (PVP), a known acid scavenger,[7d] the reaction slowed considerably. After 300 h at 165 °C in THF-$d_8$, only 4% conversion was observed. This is approximately the same as that observed at late reactions times without PVP present. It should be noted that the addition of PVP to the thermolysis of **1**, also in THF-$d_8$, did not affect the rate of the reaction.

**Thermolysis of (dppe)$PtMe_3Et$ (3).** Thermolysis of a nonequilibrium mixture of *fac* and *mer* isomers of **3** at 165 °C in benzene-$d_6$ generated the organic products ethylene, methane, ethane and propane, and the Pt(II) products (dppe)$PtMe_2$ (**6**) and (dppe)PtMeEt (**8**). The disappearance of **3** is a first-order process, with $k_{obs} = (1.2 \pm 0.1) \times 10^{-4}$ $s^{-1}$ at 165 °C. The

(34) An additional $^{31}P$ NMR signal for **6-$d_3$** may be hidden under the signals for **6** and **6-$d_6$**.

(35) Casado, A. L.; Casares, J. A.; Espinet, P. *Organometallics* **1997**, *16*, 5730 and references therein.

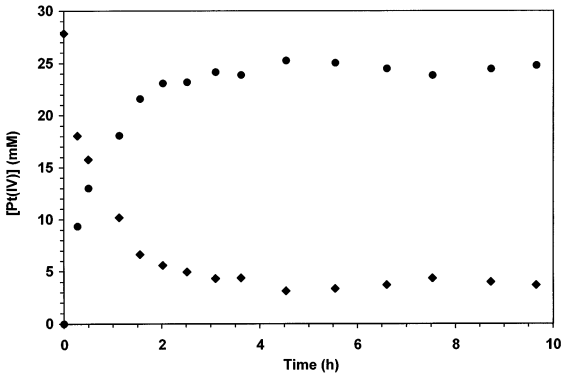


***Figure 6.*** Equilibrium plot of *fac*-**3** (♦) and *mer*-**3** (●) at 100 °C in $C_6D_6$.

***Scheme 2***

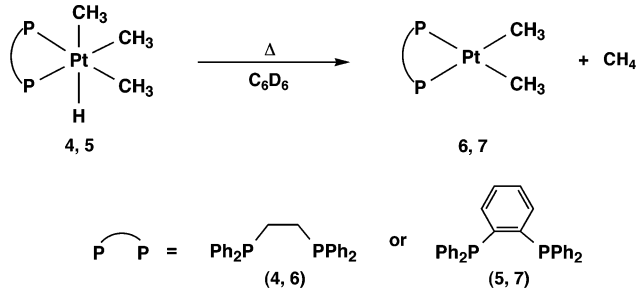


organic products were identified by $^1$H NMR (ethylene $\delta$ 5.25; methane $\delta$ 0.15; ethane $\delta$ 0.80; propane $\delta$ 0.86 (t, $^3J_{H-H} = 7$ Hz), 1.26 (m, $^3J_{H-H} = 7$ Hz)) and also by GC/MS. Analysis of the organic products by GC/FID revealed the ratio of ethylene: ethane:propane to be 75:18:7. The Pt(II) products, **6** and **8**, were identified by $^1$H and $^{31}$P NMR, and the spectra matched those of authentic samples. As determined by integration of $^1$H NMR spectra, the yields of **6** and **8** were 91% and 4%, respectively.

**Intramolecular Isomerization of 3.** During the thermolysis of **3** in benzene-$d_6$ at 165 °C, isomerization to an equilibrium mixture of *fac* and *mer* isomers was observed. At the lower temperature of 100 °C, there was no reactivity leading to organic or Pt(II) products, and the isomerization was the only process observed. The *mer* isomer is favored, with $K_{eq} = 6.3$ at 100 °C (Figure 6). The isomerization reaction was complete within 4 h, and $k_f = 3.3 \times 10^{-4}$ s$^{-1}$.[32,36] Unfortunately, purification of **3** involved column chromatography which resulted in substantial *fac* to *mer* isomerization and despite great effort, we were unable to reproducibly generate pure samples of **3** with high enough enrichment in the *fac* isomer to carry out a full kinetic/mechanistic study on the isomerization reaction.

**Thermolysis of $L_2PtMe_3H$ ($L_2$ = dppe, dppbz).** In solution, *fac*-(dppe)$PtMe_3H$ (**4**) undergoes C−H reductive elimination at ambient temperature to yield $CH_4$ and (dppe)$PtMe_2$ (**6**) (Scheme 2). The complex *fac*-(dppbz)$PtMe_3H$ (**5**) exhibits similar behavior, and produces $CH_4$ and (dppbz)$PtMe_2$ (**7**). The identities of the products were confirmed by comparison to NMR spectra of authentic samples.

The thermolyses of complexes **4** and **5** were monitored by $^1$H and $^{31}$P NMR spectroscopy in benzene-$d_6$ at 50 °C. Clean, reproducible first-order reaction kinetics were observed for both complexes. The observed rate constants for reductive elimination of methane from **4** and **5** were essentially identical, with $k_{obs} = (1.3 \pm 0.1) \times 10^{-4}$ s$^{-1}$ for complex **4**, and $k_{obs} = (1.2 \pm 0.1) \times 10^{-4}$ s$^{-1}$ for complex **5**.[32] The rates of reaction were unaffected by small amounts of (dppe)$PtMe_2$ (**6**) and (dppbz)-$PtMe_2$ (**7**) present in the starting material. The rate constants from different samples of **4** and **5** (containing variable amounts (9%−25%) of **6** and **7**, respectively) were identical.

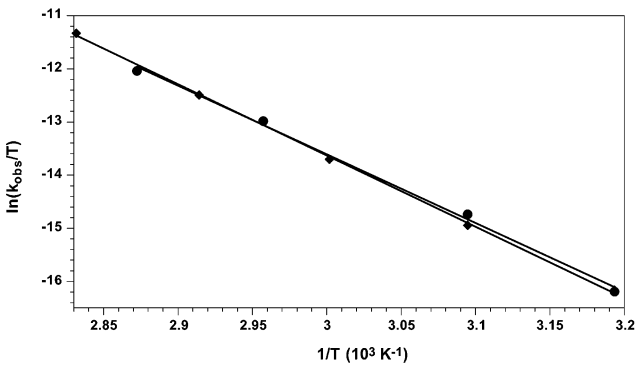


***Figure 7.*** Eyring plot for **4** (●, 40−75 °C) and **5** (♦, 40−80 °C) in $C_6D_6$.

Activation parameters for the reductive elimination of methane from **4** of $\Delta H^{\ddagger} = 25.7 \pm 1.0$ kcal/mol and $\Delta S^{\ddagger} = 3 \pm 3$ eu were calculated from kinetic data over a temperature range of 40 to 75 °C. For **5**, very similar activation parameters of $\Delta H^{\ddagger} = 26.6 \pm 0.4$ kcal/mol and $\Delta S^{\ddagger} = 6 \pm 2$ eu were found over the temperature range of 40 °C to 80 °C. The Eyring plots for the methane reductive elimination reactions from complexes **4** and **5** are shown in Figure 7.

Thermolysis of the deuteride complex **4-*d*$_1$** in benzene-$d_6$ at 50 °C led to the clean formation of **6** and $CH_3D$. Under the same reaction conditions, **5-*d*$_1$** yielded **7** and $CH_3D$. No other isotopomers of methane were observed ($^1$H NMR), and no scrambling of deuterium into Pt−Me groups of either the starting materials or of the products was detected ($^1$H, $^1$H{$^{31}$P}, and $^{31}$P NMR). Both reactions exhibited clean first-order kinetics, with similar rate constants ($k_{obs} = 5.9 \times 10^{-5}$ s$^{-1}$ for **4-*d*$_1$** and $k_{obs} = 4.8 \times 10^{-5}$ s$^{-1}$ for **5-*d*$_1$**).[32] The kinetic deuterium isotope effects for C−H(D) reductive elimination from **4** and **5** are $k_H/k_D = 2.2$ and $k_H/k_D = 2.5$, respectively.

## Discussion

**Mechanism of Ethane Elimination from (dppe)$PtMe_4$ (1).** Thermolysis of **1** in solution requires temperatures in excess of 150 °C before appreciable amounts of C−C reductive elimination to form ethane and (dppe)$PtMe_2$ (**6**) occurs. Complex **1** is significantly more thermally stable than other reported Pt(IV) trimethyl and tetramethyl complexes which undergo reductive elimination to form ethane. For example, the production of ethane from the Pt(IV) complexes $(PR_3)_2PtMe_3X$ and $(RNC)_2$-$PtMe_4$ in solution is conveniently monitored at approximately 60 °C.[7a,b] Thermolysis of $(L_2)PtMe_3X$ ($L_2$ = dppe ($PPh_2(CH_2)_2$-$PPh_2$) or dppbz (*o*-$PPh_2(C_6H_4)PPh_2$)) in solution to yield C−X and C−C reductive elimination products was studied at 79 °C for X = I, 99 °C for X = OAc, and 120 °C for X = OAr.[7c,d,g] Mechanistic investigations of C−C reductive elimination reactions from these other Pt(IV) complexes have revealed that ancillary ligand dissociation precedes the carbon−carbon bond formation step.[7] In complexes with monodentate ligands such as $PR_3$ or RNC, the neutral ligands dissociate to form a five-coordinate intermediate from which C−C coupling occurs.[7a,b]

(36) Laidler, K. J. *Chemical Kinetics*, 3rd ed.; Harper Collins: New York, 1987.

*Scheme 3*

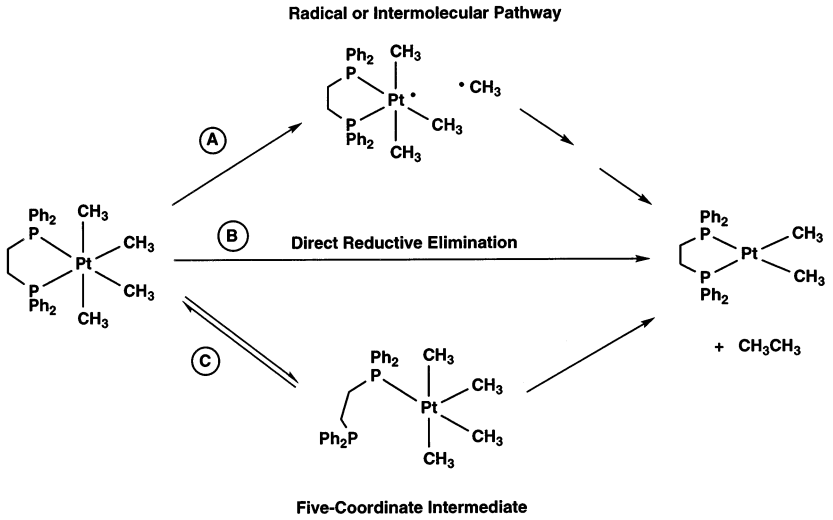


When a bidentate phosphine ligand such as dppe or dppbz is employed, a higher energy process involving charge separation occurs as dissociation of the anionic X group generates a cationic five-coordinate intermediate prior to C−C bond formation.[7c,d,g] The extraordinary kinetic stability of (dppe)$PtMe_4$ (**1**) toward reductive elimination is thus likely to result from a lack of facile access to a five-coordinate intermediate species.[7f] This is consistent with the recent report that reductive elimination of ethane from **1** can be induced to occur rapidly at room temperature by the addition of a catalytic amount of an electrophilic Pt complex.[37] The catalyst was proposed to abstract a methide group to generate the five-coordinate cationic intermediate, $dppePtMe_3^+$, from which reductive elimination takes place.

Despite the high temperatures required, the thermally promoted formation of ethane from **1** is a well-behaved first-order process. Kinetics experiments were performed between 165 and 205 °C. At 165 °C, the reaction proceeds slowly with a rate constant on the order of $4 \times 10^{-6}$ $s^{-1}$ in a variety of solvents (benzene-$d_6$, THF-$d_8$ and acetone-$d_6$). The lack of a solvent effect on the rate of the reaction is in contrast to the related thermal reductive elimination of ethane from (dppe)$PtMe_3X$ in which the rate of reaction was found to significantly increase with the polarity of the solvent.[7c,d,g] The mechanism of that reaction was shown to involve the formation of ionic intermediates.

(dppe)$PtMe_4$ (**1**) lacks both neutral monodentate ligands and a potential anionic leaving group X. Thus, both mechanisms previously established for C−C reductive elimination from Pt(IV) are disfavored. Three reasonable alternative mechanisms for the reductive elimination of ethane from the Pt(IV) tetramethyl complex **1** can then be considered (Scheme 3).

The first mechanism is a radical or intermolecular pathway (A). With estimates of $Pt^{IV}$−C bond strengths of 30−37 kcal/mol[7a−c,38] and temperatures in excess of 150 °C required for reductive elimination, a Pt−Me bond cleavage pathway appears reasonable. However, evidence against mechanism A is provided by the results of the crossover study. When **1** and **1-*d*$_{12}$** were heated at 165 °C for just over one half-life, < 4% of the crossover product, $CH_3CD_3$, was observed. Thus, the major pathway for ethane elimination from **1** involves an intramolecular reaction, rather than a radical or other intermolecular process.

The two intramolecular mechanisms to be considered are direct elimination (pathway B) and chelate opening to form a five-coordinate intermediate prior to C−C coupling (pathway C). The latter pathway is analogous to the neutral ligand predissociation mechanism observed with monodentate ligands. However, in contrast to the situation with monodentate ligands, the chelate remains coordinated ($\kappa^1$). Thus, paths B and C are kinetically indistinguishable and both mechanisms should yield first-order rate laws. Nevertheless, the measured activation entropy for the reaction potentially provides some insight to differentiate between the two mechanisms. The fairly large $\Delta S^{\ddagger}$ value (15 ± 4 eu) is more consistent with pathway C, a reversible chelate opening (ligand dissociation) prior to reductive coupling. A value closer to zero would be expected for pathway B (see data for reductive elimination from **4** and **5)**, and potentially for pathway C if chelate-opening was rate-determining. Yet, it should be noted that had a $\Delta S^{\ddagger}$ value close to zero actually been observed, the interpretation would have been more ambiguous. A survey of the literature shows that despite similar proposed reaction mechanisms, i.e., ancillary ligand dissociation, $\Delta S^{\ddagger}$ values previously reported for C−C reductive elimination reactions from Pt(IV) alkyl complexes vary over a considerable range (−21 to +44 eu, Table 4). Even within the closely related series of complexes $(PMe_2Ph)_2PtMe_3X$ (X = Cl, Br, I) which all undergo reaction by preliminary phosphine dissociation, the values vary from 4 ± 2 eu for X = Cl up to 16 ± 1 eu for X = I.

More compelling evidence against the direct elimination pathway (B) was provided by thermolysis of the closely related complex, (dppbz)$PtMe_4$ (**2**). The two bidentate phosphine ligands, dppe and dppbz, are very similar in the sterics and electronics of their binding to Pt(IV). The P−Pt−P bond angles for dppe and dppbz are nearly identical; the P−Pt−P angle is 86° in (dppe)$PtMe_4$ (**1**), and 84° in (dppbz)$PtMe_4$ (**2**). These values are consistent with literature reports for other complexes.[39] The platinum−phosphorus coupling constants for the two complexes are almost identical (1145 Hz for **1** and 1147 Hz for **2**). Little difference is also noted in the $PtMe_4$ fragments of these two complexes. The Pt−C bond lengths are very similar

(37) Hill, G. S.; Yap, G. P. A.; Puddephatt, R. J. *Organometallics* **1999**, *18*, 1408.

***Table 4.*** Literature Values of $\Delta S^{\ddagger}$ for Ethane Elimination from Pt(IV)

| complex | $\Delta S^{\ddagger}$ (cal/mol K) | solvent | mechanism proposed | ref |
|---|---|---|---|---|
| $(MeNC)_2PtMe_4$ | $-21 \pm 3$ | benzene | isonitrile dissociation | 7b |
| $(PMe_2Ph)_2PtMe_3Cl$ | $4 \pm 2$ | 1,4-dioxane | phosphine dissociation | 7a |
| $(PMe_2Ph)_2PtMe_3Br$ | $11 \pm 1$ | 1,4-dioxane | phosphine dissociation | 7a |
| $(PMe_2Ph)_2PtMe_3I$ | $16 \pm 1$ | 1,4-dioxane | phosphine dissociation | 7a |
| $(PMePh_2)_2PtMe_3I$ | $44 \pm 4$ | 1,4-dioxane | phosphine dissociation | 7a |

(Table 2) and the $J_{P-H}$ coupling constants for the Pt(IV)-$CH_3$ groups are nearly identical (for Me trans to Me, $J_{P-H} = 6.4$ Hz in **1** and 5.9 Hz in **2**; for Me trans to P, $J_{P-H} = 6.8$ Hz in both **1** and **2**) Thus, the electron donating ability of these two phosphine ligands appears to be comparable.

The most significant difference between dppe and dppbz ligands is the flexibility of the backbone. The benzene backbone of dppbz is considerably more rigid than the ethane backbone of dppe. The relative flexibility of the phosphine chelate should become important in reactions in which one end of the phosphine chelate dissociates from the metal center. Differences in phosphine chelate flexibility have been previously used in attempts to probe possible phosphine dissociation in C−X (X = CN, SR) reductive eliminations from Pd(II) complexes.[40] The flexibility of the phosphine chelate had no effect in these Pd(II) systems, a result which was used to support direct eliminations not requiring chelate opening (phosphine predissociation). Similarly in a Pt(IV) system closely related to that under discussion here, C−O reductive elimination reactions from $(dppe)PtMe_3OAc$ and $(dppbz)PtMe_3OAc$ were found to have the same rate constant, despite the different phosphines.[7g] The mechanism for these Pt(IV) reductive elimination reactions was found to involve initial dissociation of acetate, rather than phosphine. The reductive elimination of ethane from $(dppe)PtMe_4$ (**1**) is unique in that a very large effect on reactivity was observed as a result of varying the phosphine chelate flexibility. Thermolysis of $(dppbz)PtMe_4$ (**2**), which has the less flexible phosphine, showed only 4% conversion after 300 h at 165 °C in THF-$d_8$. To achieve 4% conversion of $(dppe)PtMe_4$ (**1**) (a first-order process) would require only ca. 3.5 h under the same conditions. This ca. 100-fold difference between the rates of ethane reductive elimination from **1** and **2** correlates with phosphine chelate flexibility and provides strong support for a mechanism involving phosphine dissociation prior to C−C coupling for complex **1** (pathway C).

Evidence has also been obtained to show that mechanism C is kinetically viable. That is, phosphine chelate opening does occur, and it does so on a time scale that would allow it to precede the C−C coupling reaction. The observation of $\beta$−hydride elimination products upon thermolysis of the closely related tetraalkyl complex $(dppe)PtMe_3Et$ (**3**) at 165 °C establishes that the phosphine dissociation to generate an open site takes place readily at this temperature. $\beta$−hydride elimination requires an open coordination site cis to the ligand with $\beta$−hydrogens.[1] Upon thermolysis of **3** in benzene-$d_6$ at 165 °C, the organic products ethylene, methane, ethane and propane were observed. The ratio of ethylene to propane to ethane was 75:18:7 indicating that while $\beta$−hydride elimination dominates, C−C reductive elimination to form propane and ethane is competitive.

***Scheme 4***

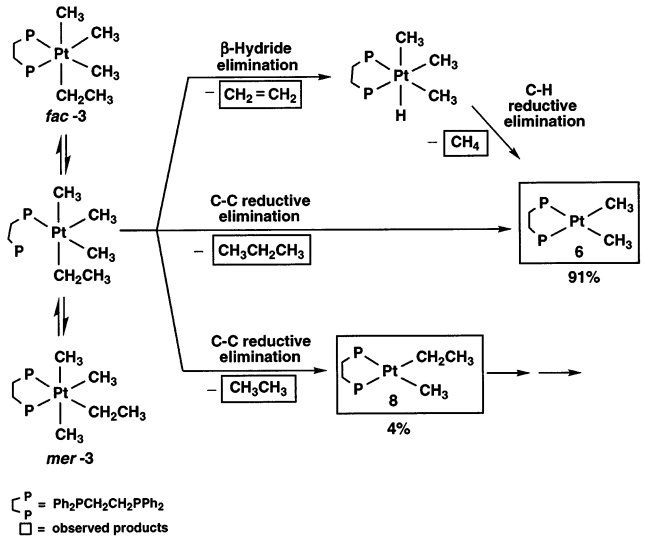


The mechanism most consistent with the formation of these products from **3** is shown in Scheme 4. Dissociation of phosphine to yield a five-coordinate intermediate occurs as the first step. The $\beta$−hydride elimination reaction proceeds from the five-coordinate intermediate to generate ethylene and the Pt(IV) methyl hydride complex, $(dppe)PtMe_3H$ (**4**). Complex **4** undergoes C−H reductive elimination at ambient temperature (as described above), and therefore should undergo rapid elimination of methane at 165 °C. The final Pt product from this pathway is $(dppe)PtMe_2$ (**6**). Competitive with $\beta$−hydride elimination, presumably from the five-coordinate intermediate, is C−C reductive elimination to form propane and $(dppe)PtMe_2$ (**6**) or ethane and the Pt(II) methyl ethyl complex (dppe)PtMeEt (**8**)**.** The Pt(II) complex **8** is a 16 $e^-$ species and could itself undergo $\beta$−hydride elimination to generate ethylene and Pt(0).[41] However, any such reactivity would be a minor contribution, as 95% of the Pt was accounted for as tractable Pt(II) products (91% of **6,** 4% of **8)**. Thus, the majority of the ethylene results from $\beta$−hydride elimination from the Pt(IV) species **3** rather than the Pt(II) complex **8**.

Additional support for the kinetic competence of the phosphine dissociation pathway is provided by the isomerization of **3** to an equilibrium mixture of *fac* and *mer* isomers during the thermolysis at 165 °C. At 100 °C, isomerization of **3** occurs cleanly without further reaction to generate Pt(II) complexes (Figure 6). Isomerization of octahedral Pt(IV) complexes is most commonly proposed to occur via fluxional five-coordinate

(38) Low, J. J.; Goddard, W. A. *J. Am. Chem. Soc.* **1986**, *108*, 6115.
(39) Dierkes, P.; van Leeuwen, P. W. N. M. *J. Chem. Soc., Dalton Trans.* **1999**, 1519, and references therein.
(40) (a) Mann, G.; Baranano, D.; Hartwig, J. F.; Rheingold, A. L.; Guzei, I. A. *J. Am. Chem. Soc.* **1998**, *120*, 9205. (b) Marcone, J. E.; Moloy, K. G. *J. Am. Chem. Soc.* **1998**, *120*, 8527.
(41) Bryndza, H. E.; Calabrese, J. C.; Marsi, M.; Roe, C. D.; Tam, W.; Bercaw, J. E. *J. Am. Chem. Soc.* **1986**, *108*, 4805, and references therein.

intermediates.[20b,42] The long assumed high fluxionality of five-coordinate Pt(IV) was recently supported by the observation that the isolable five-coordinate Pt(IV) complex (nacnac)$PtMe_3$ remains fluxional down to at least −50 °C.[9a] Isomerization of **3** is thus proposed to proceed via a five-coordinate intermediate formed by dissociation of one end of the phosphine chelate (Scheme 4).

An interesting observation is made when comparing the thermolyses reactions of **1** and **3**. The C−C reductive elimination reaction of two methyl groups to form ethane is faster from **3** than from **1**. The rate constant for ethane formation from **1** is $4.2 \times 10^{-6}$ $s^{-1}$ (165 °C, $C_6D_6$), whereas the estimated rate constant for ethane elimination from **3** is $8.4 \times 10^{-6}$ $s^{-1}$ (165 °C, $C_6D_6$).[43] Given that Me−Me coupling is statistically twice as likely from **1** than from **3**, the reductive elimination of ethane is actually four times faster from **3** than from **1**. This acceleration of Me−Me coupling in the presence of an ethyl group can easily be accommodated by a mechanism involving phosphine dissociation occurring prior to rate-determining C−C reductive elimination. Under these conditions (Path C, Scheme 3), the equilibrium constant for phosphine dissociation ($K_{phos}$) will factor into the observed rate constant for the Me−Me coupling. The presence of an ethyl group should lead to a greater value of $K_{phos}$ on both steric and electronic grounds. The sterically bulkier ethyl group should favor phosphine dissociation. In addition, the Pt−P coupling constant observed for the phosphorus trans to ethyl in ***mer*-3** ($^1J_{Pt-P} = 992$ Hz), as compared to that trans to methyl ($^1J_{Pt-P} = 1141$ Hz), clearly illustrates that ethyl is a stronger trans influence ligand than methyl. The tetramethyl complex **1** has $^1J_{Pt-P} = 1145$ Hz for phosphorus trans to methyl. Thus, the phosphine trans to the ethyl group in ***mer*-3** appears to be more weakly bound to the Pt metal center than that trans to a methyl group, and a greater $K_{phos}$ is expected for **3** than for **1**.[44] This greater $K_{phos}$ should yield a larger $k_{obs}$ for Me−Me coupling.

It was also noted in the thermolysis of **3** at 165 °C, that Me−Et elimination to form propane was preferred over Me−Me elimination to form ethane. Statistically, equal amounts of propane and ethane are expected. Instead, the observed ratio of propane to ethane was 2.5:1. A similar preference for ethyl versus methyl coupling reactions was reported for the thermolysis of $(PMe_2Ph)_2PtMeEt_2I$ in which Et−Et coupling to form butane was observed, but no Me−Et coupling to form propane was detected.[45] The preference for C−C reductive elimination of propane from **3** could be a simple steric effect or it may be due to the stronger trans influence of the ethyl ligand versus the methyl ligand. Dissociation of the phosphine trans to ethyl places the ethyl ligand in the apical position of the resulting five-coordinate square-pyramidal complex. Concerted C−C (and C−H) reductive elimination occurs with the apical ligand and one of the basal ligands.[25,46] If the placement of the ethyl ligand in the apical position of the five-coordinate intermediate is favored thermodynamically on the basis of its stronger trans influence, then reductive coupling of the ethyl ligand with a basal methyl ligand may occur with greater frequency than methyl−methyl coupling.

Given the discussion above which indicates that the proclivity for phosphine dissociation (chelate opening) appears to be greater for (dppe)$PtMe_3Et$ (**3**) versus (dppe)$PtMe_4$ (**1**), it is natural to question whether **3** is truly a sufficient model for **1** in terms of establishing the kinetic viability of phosphine dissociation occurring on the C−C reductive elimination pathway. A more direct analogue of **1** is the partially deuterated tetramethyl complex (dppe)$PtMe(CD_3)_3$ (***fac*-1-$d_9$**). Although *fac/mer* isomerization was indeed observed when ***fac*-1-$d_9$** was heated at 100 °C in benzene-$d_6$, the reaction proceeded almost 200 times more slowly than the isomerization of ***fac*-3**. This large disparity in the rates of isomerization of ***fac*-1-$d_9$** and ***fac*-3** can be attributed to a combination of the differences in rates of phosphine chelate opening and the rates of isomerization of the respective five-coordinate intermediates. However, the important point to be noted here is that both of these isomerization reactions are significantly faster than C−C reductive elimination. Thus, even though isomerization of ***fac*-1-$d_9$** at 100 °C is a relatively slow process ($k_f = 1.7 \times 10^{-6}$ $s^{-1}$), the rate constant for ethane elimination from **1** at 100 °C, as estimated from the Eyring plot (Figure 2), is $6.8 \times 10^{-10}$ $s^{-1}$, which is 2500 times slower than isomerization.

**Mechanism of Methane Elimination from $L_2PtMe_3H$ ($L_2$ = dppe, dppbz).** Similar to C−C reductive elimination of alkyl groups from Pt(IV), previous studies of C−H reductive elimination of alkanes from Pt(IV) have provided evidence for ancillary ligand dissociation and C−H coupling from a five-coordinate intermediate.[20−22,47] However, all of these experimental studies have involved Pt(IV) alkyl hydride complexes with nitrogen donor ligands. Recently, calculations in phosphine ligated systems have been used to examine the possibility of direct C−H reductive elimination.[46,48] In calculations using the model complex $Cl_2(PH_3)_2Pt(CH_3)H$, reductive elimination of methane was found to occur preferentially via a five-coordinate intermediate formed by preliminary phosphine dissociation.[46] No transition state for the direct elimination pathway could even be found. When phosphine dissociation was disfavored by using the more basic phosphine $PMe_3$, a significant difference was noted. Direct reductive elimination of methane from $Cl_2(PMe_3)_2Pt(CH_3)H$ was found to be enthalpically *favored* by 2 kcal/mol over a phosphine dissociation pathway.[48] However, the entropy associated with phosphine dissociation cannot be neglected, and would likely overcome, in practice, the slight enthalpic preference for direct elimination. In contrast, with a chelating phosphine, the entropic advantage of phosphine dissociation would be significantly reduced and it was suggested that a Pt(IV) alkyl hydride complex with a chelating phosphine ligand might undergo direct C−H reductive elimination.

The effect of using a chelating phosphine on the stability of $L_2PtMe_3H$ is indeed dramatic. *fac*-(dppe)$PtMe_3H$ (**4**) and *fac*-(dppbz)$PtMe_3H$ (**5**) are the first alkyl hydride complexes of Pt(IV) bearing phosphine ligands that have been isolated.[24] **4**

(42) (a) Crespo, M.; Puddephatt, R. J. *Organometallics* **1987**, *6*, 2548. (b) Wehman-Ooyevaar, I. C. M.; Drenth, W.; Grove, D. M.; van Koten, G. *Inorg. Chem.* **1993**, *32*, 3347, and references therein.

(43) This number was calculated by multiplying the observed rate constant for thermolysis of (dppe)$PtMe_3Et$ at 165 °C ($k_{obs} = 1.2 \times 10^{-4}$ $s^{-1}$) by the relative percent ethane formation (7%) from the GC/FID analysis.

(44) Note that the ***fac*-3**/***mer*-3** equilibrium favors the *mer* isomer, and this equilibrium is established rapidly.

(45) Brown, M. P.; Puddephatt, R. J.; Upton, C. E. E.; Lavington, S. W. *J. Chem. Soc., Dalton Trans.* **1974**, 1613.

(46) Bartlett, K. L.; Goldberg, K. I.; Borden, W. T. *J. Am. Chem. Soc.* **2000**, *122*, 1456, and references therein.

(47) With chelating ligands, although ligand dissociation (chelate-opening) has been proposed, whether ligand dissociation occurs prior to or concurrent with the C−H coupling is difficult to determine.

(48) Bartlett, K. L.; Goldberg, K. I.; Borden, W. T. *Organometallics* **2001**, *20*, 2669.

***Scheme 5***

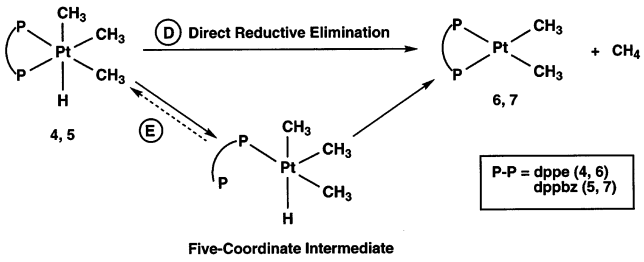


has even been crystallographically characterized. Both **4** and **5** undergo C−H reductive elimination to form methane at ambient temperature. Similar to C−C reductive elimination from the tetramethyl analogue **1**, both a direct elimination pathway (D) and a chelate opening (ligand dissociation) pathway (E) are considered as possible mechanisms for the C−H reductive elimination reaction (Scheme 5).

The phosphine dissociation pathway (E) would be analogous to the mechanism supported for C−C reductive elimination from (dppe)$PtMe_4$ (Pathway C, Scheme 3), as described above. The most convincing evidence for the involvement of phosphine dissociation in the C−C reductive elimination reaction from **1** was the dramatic rate inhibition that occurred when dppe was replaced by the more rigid chelating ligand dppbz. In contrast, C−H reductive elimination reactions from *fac*-(dppe)$PtMe_3H$ (**4**) and *fac*-(dppbz)$PtMe_3H$ (**5**) both proceed with virtually identical first-order rate constants (ca. $1 \times 10^{-4}$ $s^{-1}$ at 50 °C in benzene-$d_6$) and have very similar activation parameters ($\Delta H^{\ddagger} \approx 26$ kcal/mol, $\Delta S^{\ddagger} \approx 3-6$ eu). The similarity in the rates and activation parameters for the complexes of dppe and the more rigid chelate dppbz provide compelling support for a mechanism of direct elimination, without prior ligand dissociation (Pathway D).

A $\Delta S^{\ddagger}$ value close to zero would be expected for a direct elimination and so the relatively low values of $\Delta S^{\ddagger}$ observed for methane elimination from **4** and **5** would be consistent with a mechanism that does not involve initial chelate opening. Yet, it is important to note that the small $\Delta S^{\ddagger}$ values do not preclude a chelate-opening mechanism. Particularly, if the chelate-opening were the rate-determining step, the resulting increase in entropy might not be realized in the transition state. Similar to C−C reductive elimination reactions, examination of $\Delta S^{\ddagger}$ for a variety of C−H reductive elimination reactions from $d^6$ late transition metal complexes shows that the values span a considerable range, particularly for those reactions proposed to proceed via ligand dissociation pathways (Table 5). It is, however, difficult to reconcile a chelate-opening step (rate-determining or otherwise) with the observation of virtually identical activation parameters (both $\Delta H^{\ddagger}$ and $\Delta S^{\ddagger}$) for dppe and dppbz, in view of the fact that the chelates are of such differing rigidity. In addition, the fact that C−H reductive elimination is completely independent of the rigidity of the chelate, whereas C−C reductive elimination is extremely sensitive to this parameter, strongly argues (even more so than does each observation individually) that the C−C elimination, but not the C−H eliminations, proceeds via chelate-opening. In light of this difference in mechanism, the significantly different values of $\Delta S^{\ddagger}$ for C−C reductive elimination ($15 \pm 4$ eu) and for C−H reductive elimination (3−6 eu) appear quite reasonable.

The deuterium isotope effects for C−H(D) reductive elimination from **4** and **5** are both normal (>1), and are similar for both complexes. The kinetic isotope effect for C−H(D) coupling from **4** was $k_H/k_D = 2.2$, and from **5** was $k_H/k_D = 2.5$. The isotope effects measured for **4** and **5** do not help to distinguish between the possible mechanisms of direct elimination and phosphine dissociation, as both normal and inverse isotope effects have been observed for C−H eliminations from transition metal alkyl hydrides occurring by both paths.[20a] The normal isotope effects for C−H reductive elimination from **4** and **5** do, however, confirm that C−H coupling is the rate-determining step.

**C−C vs C−H Reductive Elimination from $L_2PtMe_3R$ ($L_2$ = dppe, dppbz; R = Me, H).** The series of complexes ($L_2PtMe_3R$; $L_2$ = dppe, dppbz; R = Me, H) provide a unique opportunity to directly compare Me−Me and Me−H reductive elimination reactions.[49] For the first time, both reactions are observed from the same metal ligand environment. Typically, if C−H reductive elimination is observed from a metal alkyl hydride complex, the analogous metal dialkyl complex is stable to C−C reductive elimination.[50] Often, other decomposition pathways are found to dominate upon thermolysis of the metal dialkyl species.[50a,c] Conversely, for those systems in which C−C reductive elimination is observed, the corresponding metal alkyl hydrides are too unstable, even at low temperatures, to allow for adequate mechanistic study.

Indeed, in the Pt(IV) bisphosphine system described here, a dramatic temperature difference for reductive elimination from the trialkyl hydride complexes versus the tetramethyl complexes is observed. The $L_2PtMe_3H$ complexes undergo reductive elimination of methane at 50 °C, with $k_{obs} = 1 \times 10^{-4}$ $s^{-1}$. To achieve a comparable rate constant for C−C reductive elimination from (dppe)$PtMe_4$ (**1**), a temperature of nearly 200 °C (extrapolation from the Eyring data) would be required. However, perhaps even more significant than the difference in rates of reaction is that C−C and C−H reductive elimination proceed via different mechanisms. C−H reductive elimination from *fac*-(dppe)$PtMe_3H$ (**4**) and *fac*-(dppbz)$PtMe_3H$ (**5**) proceeds directly from the six-coordinate geometry. C−C reductive elimination from (dppe)$PtMe_4$ (**1**) has a much higher activation barrier and does not proceed via a direct coupling pathway. Rather, dissociation of one end of the phosphine chelate occurs and C−C coupling takes place from a five-coordinate species.

Calculations have confirmed that C−H and C−C coupling reactions are more facile from five-coordinate Pt(IV) centers than from the six-coordinate complexes.[46,48] However, the enthalpic cost of ligand dissociation must also be considered. When the entropic advantage of ligand loss is thwarted by employment of a chelating ligand, then direct elimination may become feasible. C−H reductive elimination has, in general, a lower activation barrier than C−C reductive elimination, and with a chelating phosphine C−H reductive elimination from Pt(IV) occurs directly from the six-coordinate species. The enthalpic barrier to C−C reductive elimination is significantly higher and C−C coupling apparently does not take place from

(49) Norton, J. R.; *Acc. Chem. Res*. **1979**, *12*, 139. (b) Glueck, D. S.; Bergman, R. G. *Organometallics* **1991**, *10*, 1479 (c) Rees, W. M.; Churchill, M. R.; Li, Y.-J.; Atwood, J. D. *Organometallics* **1985**, *4*, 1162.

(50) For example: (a) Cp*$(PMe_3)Ir(Me)(H)$ versus Cp*$(PMe_3)Ir(Me)_2$, ref 49b (b) $MeIr(H)_2(CO)(PPh_3)_2$ versus $Me_2Ir(CO)(PPh_3)_2I$, ref 49c (c) $(N_2)PtMe_2(H)X$ versus $(N_2)PtMe_3X$ where $N_2$ = bpy or tmeda, refs 13b, 20a, 21, 25.

***Table 5.*** Literature Values of $\Delta S^{\ddagger}$ for C−H Elimination from Pt(IV), Ir(III) and Rh(III)

| compound | $\Delta S^{\ddagger}$ (eu) | *T* (K)/solvent | mechanism proposed | ref |
|---|---|---|---|---|
| (tmeda)Pt($CH_2Ph$)$HCl_2$ | −18.5 | 230−249, $CD_2Cl_2$ | $Cl^-$ dissoc. | 20a |
| (tmeda)Pt$Me_2$HCl | 4.1 | 238−258, $CD_3OH$ | $Cl^-$ dissoc. | 20a |
| *cis*-[(BPMA)Pt$Me_2$H]$BF_4$[a] | 6.7 | 293−313, $CD_2Cl_2$ | pyridyl dissoc. | 20c |
| *trans*-[(BPMA)Pt$Me_2$H]$BF_4$[b] | 24.1 | 298−311, $CD_2Cl_2$ | pyridyl dissoc. | 20c |
| $Tp^{Me2}PtMe_2H$ | 13 | 363−403, $C_6D_6$ | pyrazolyl dissoc. | 20h |
| (dppe)(CO)Ir$EtH_2$ | −10.9 | 291−317, $C_6D_6$ | direct elim. | 16c |
| $Cp^*(PMe_3)Ir(C_6H_{11})H$ | 10 | 398−413, $C_6D_6$ | direct elim. | 16b |
| $(PMe_3)_3Rh(CH_2OMe)HCl$ | 5.3 | 300−317 $C_6D_6$ | $PMe_3$ dissoc. | 17a |

[a] The hydride is cis to the amine ligand of BPMA. [b] The hydride is trans to the amine ligand of BPMA.

the six-coordinate complex. Rather a lower energy route involving ligand loss is followed. Despite this lower energy pathway, the C−C coupling still requires a temperature some 150 °C higher than the C−H reductive elimination reaction. Thus, although theoretically possible, direct $sp^3$C-$sp^3$C reductive elimination from six-coordinate Pt(IV) without preliminary ligand dissociation appears to be an unfavorable reaction pathway.

## Summary

The Pt(IV) complex (dppe)$PtMe_4$ (**1**) undergoes reductive elimination of ethane at very high temperatures in solution. Despite the chelate effect of dppe, considerable evidence supports that reductive elimination from **1** proceeds via a mechanism that involves dissociation of one end of the phosphine chelate to form a five-coordinate intermediate prior to C−C bond formation (pathway C, Scheme 3). Replacing the chelating bisphosphine dppe with the more rigid bisphosphine chelate dppbz results in a dramatic reduction in the rate of ethane elimination; reductive elimination of ethane from (dppbz)$PtMe_4$ (**2**) is 2 orders of magnitude slower than from **1**. The observation of isomerization of *fac*-(dppe)$PtMe_3Et$ (**3**) and *fac*-(dppe)Pt$Me(CD_3)_3$ (***fac*-1-*d*$_9$**) at a significantly lower temperature, in conjunction with $\beta$-hydride elimination from (dppe)$PtMe_3Et$ (**3**), demonstrates the kinetic viability of dppe chelate opening prior to C−C coupling.

The novel Pt(IV) alkyl hydride complexes *fac*-(dppe)$PtMe_3H$ (**4**) and *fac*-(dppbz)$PtMe_3H$ (**5**) were found to undergo C−H reductive elimination of methane at ambient temperature in solution. **4** and **5** are the first examples of Pt(IV) alkyl hydrides ligated by phosphorus which are stable enough to be isolated and **4** has been crystallographically characterized. In contrast to the C−C reductive elimination reactions from the analogous complexes **1** and **2**, C−H reductive elimination reactions from **4** and **5** occur at virtually identical rates with similar activation parameters. The similarity of the facility of the reaction irrespective of the rigidity of the phosphine chelate strongly supports the proposal that these reactions occur directly from the six-coordinate geometry. This is the first time that mechanistic evidence for the direct reductive elimination of alkanes from octahedral Pt(IV) alkyl complexes has been reported.

## Experimental Section

**General Information.** Unless otherwise noted, all reactions under nitrogen were carried out in a Vacuum Atmospheres VAC-MO-40-M drybox. Samples were weighed using a Mettler-Toledo B154 College analytical balance. Outside the box, samples were weighed using a Mettler-Toledo AG204 DeltaRange analytical balance. Samples requiring microgram accuracy were weighed on a Mettler MT5 analytical balance. Elemental analyses were carried out by either Canadian Microanalytical Services Ltd., Delta, B. C., Canada or Atlantic Microlab, Inc., Norcross, GA.

$^1$H NMR spectra were collected using Bruker AC 200, DPX 200, AF 301, DRX 499, and AM 500 spectrometers. The spectra were referenced to residual protiated solvent and chemical shifts are reported in parts per million downfield of tetramethylsilane. $^{13}C\{^1H\}$ NMR spectra were collected using Bruker DRX 499 (125 MHz) and AM 500 (125 MHz) spectrometers. The spectra were referenced to residual protiated solvent peaks or a known chemical shift standard. Chemical shifts are reported in parts per million downfield of tetramethylsilane. $^{31}P\{^1H\}$ NMR spectra were collected using Bruker AC 200 (81 MHz), DPX 200 (81 MHz), AF 301 (121.5 MHz) and AM 500 (202.5 MHz) spectrometers. The spectra were referenced to an external standard of 85% phosphoric acid, and chemical shifts are reported in parts per million downfield from this reference. All coupling constants are reported in Hertz.

NMR tube reactions were carried out in flame-sealed Wilmad 504-PP medium-walled tubes. Sealed tubes were prepared either using a tube previously attached to a ground glass joint or by attaching the tube to a Kontes vacuum stopcock via a Cajon adapter.[51] The volume of the solution in the tube was measured by comparison to a previously calibrated 504-PP tube. As a safety precaution, the tubes were surrounded by stainless steel jacket tubes during heating and rapid cooling. The oil bath used for heating was a Neslab Excal EX-250 HT elevated temperature bath.

The crossover study was carried out in a Wilmad pressure/vacuum valve tube (524-PV-7). The tube was attached to a Kontes vacuum stopcock via Swagelok and Cajon fittings. The gases produced were analyzed by a Kratos direct insertion mass spectrometer.

The gases produced in the thermolysis of (dppe)$PtMe_3Et$ were analyzed by injection into a Kratos mass spectrometer fitted with a Chrompack plot fused silica capillary column (50 in × 0.53 mm ID, 30 ft) with an alumina/KCl coating. The injector temperature was 50 °C, the oven was cooled to 0 °C, and the source temperature was 200 °C. The relative amount of each gas was determined by injection into a Hewlett-Packard GC/FID fitted with the same Chrompack column, with the oven cooled to 10 °C and a flow rate of 4 psi. The syringe used for these experiments was a 50 $\mu$L Gastight syringe with a locking valve.

Unless otherwise specified, all reagents were purchased from commercial suppliers and used without further purification. The phosphines [dppe ($PPh_2(CH_2)_2PPh_2$) and dppbz (*o*-$PPh_2(C_6H_4)PPh_2$)] were recrystallized before use. Toluene, ether, and THF were distilled under nitrogen from sodium/benzophenone. Pentane was distilled under nitrogen from $CaH_2$. Dioxane, benzene-$d_6$, and THF-$d_8$ were vacuum transferred from sodium/benzophenone. Acetone-$d_6$ and hexamethyldisiloxane were vacuum transferred from activated 4Å sieves. $[PtMe_3I]_4$[52] and (dppe)$PtMe_3I$[7c] were prepared as previously described. The deuterated analogues of these compounds were prepared in the same manner, with deuterated alkylating reagents substituted for the protiated

(51) Wayda, A. L.; Darensbourg, M. Y. *Experimental Organometallic Chemistry: A Practicum in Synthesis and Characterization*; ACS Symposium Series 357; American Chemical Society: Washington, DC, 1987.
(52) Clark, H. C.; Manzer, L. E. *J. Organomet. Chem.* **1973**, *59*, 411.

versions. (dppe)$PtMe_3(OAc)$[7d] and (dppbz)$PtMe_3(OAc)$[7e] were prepared as previously described.

**Synthesis, Purification and Characterization of (dppe)$PtMe_4$ (1).** An alternative preparation to that previously reported for **1** was used.[30] Under nitrogen, an ether solution of $CH_3Li$ (11 mL, 15 mmol) was added dropwise with stirring to a cooled suspension (−35 °C) of (dppe)-$PtMe_3I$ (394 mg, 0.515 mmol) in toluene (15 mL). The reaction was allowed to come to ambient temperature, and after stirring overnight, the solution was pale yellow and slightly cloudy. In the air, water (2 mL) was added dropwise to the reaction mixture (0 °C). The volatiles were removed under vacuum and toluene (20 mL) was added to the flask to separate the organometallic product from the inorganic salts. The mixture was filtered through pipets packed with glass wool, and the volatiles were removed from the filtrate, which left behind a pale yellow oil. **1** was separated from the (dppe)$PtMe_2$ (**6**) byproduct of the reaction via chromatography on neutral alumina. **1** was eluted with 3:1 pentane/$CH_2Cl_2$ and pure $CH_2Cl_2$ was used to elute **6**. The fractions containing only **1** (determined by TLC and/or NMR) were combined and evaporated to dryness. Recrystallization from $CH_2Cl_2$/pentane afforded colorless needles in 60% yield (0.202 mg). $^1$H NMR: ($C_6D_6$) $\delta$ 0.14 (t, w/Pt satellites, 6H, $^2J_{Pt-H} = 44$, $^3J_{P-H} = 6.4$, Pt−C$H_3$ trans to methyl), 1.6 (t, w/Pt satellites, 6H, $^2J_{Pt-H} = 60$, $^3J_{P-H} = 6.9$, Pt−C$H_3$ trans to phosphorus), 2.2 (m, 4H, P−C$H_2$–C$H_2$–P), 7.0−7.4 (complex pattern, aromatic signals); (THF-$d_8$) $\delta$ −0.54 (t, w/Pt satellites, 6H, $^2J_{Pt-H} = 44$, $^3J_{P-H} = 6.4$, Pt−C$H_3$ trans to methyl), 0.82 (t, w/Pt satellites, 6H, $^2J_{Pt-H} = 60$, $^3J_{P-H} = 6.8$, Pt−C$H_3$ trans to phosphorus), 2.8 (m, 4H, P−C$H_2$–C$H_2$–P), 7.2−7.7 (complex pattern, aromatic signals). $^{13}$C NMR ($C_6D_6$): $\delta$ −4.6 (s, w/Pt satellites, $^1J_{Pt-C} = 398$, Pt-$CH_3$ trans to methyl), 3.4 (dd, w/Pt satellites, $^1J_{Pt-C} = 547$, *trans*-$^2J_{P-C} = 127$, *cis*-$^2J_{P-C} = 4.9$, Pt-$CH_3$ trans to phosphorus), 28.6 (complex pattern, P-$CH_2$–$CH_2$–P), 128−134 (aromatic signals, unresolved). $^{31}$P NMR data: ($C_6D_6$) $\delta$ 7.3 (s, w/Pt satellites, $^1J_{Pt-P} = 1145$); (acetone-$d_6$) $\delta$ 7.7 (s, w/Pt satellites, $^1J_{Pt-P} = 1176$); ($CDCl_3$) $\delta$ 6.8 (s, w/Pt satellites, $^1J_{Pt-P} = 1151$). Elemental analysis calculated for $C_{30}H_{36}P_2Pt$: C, 54.90; H, 5.33. Found: C, 55.13; H, 5.55.

**Synthesis, Purification and Characterization of (dppe)$Pt(CD_3)_4$ (1-$d_{12}$).** Under nitrogen, an ether solution of $CD_3Li$ (9 mL, 4.5 mmol) was added dropwise with stirring to a cooled suspension (−35 °C) of (dppe)$Pt(CD_3)_3I$ (151 mg, 0.195 mmol) in toluene (10 mL). The rest of the procedure used to isolate and purify **1-$d_{12}$** is identical to that reported above for **1**. Colorless needles of **1-$d_{12}$** were isolated in 51% yield (66.2 mg). $^1$H NMR ($C_6D_6$): $\delta$ 2.2 (m, 4H, P−C$H_2$–C$H_2$–P), 6.9−7.5 (complex aromatic region). $^{31}$P NMR ($C_6D_6$): $\delta$ 7.4 (s, w/Pt satellites, $^1J_{Pt-P} = 1145$).

**Synthesis, Purification and Characterization of *fac*-(dppe)$PtMe(CD_3)_3$ (*fac*-1-$d_9$).** Under nitrogen, a THF solution of MeMgCl (2 mL, 5.6 mmol) was added to a suspension of (dppe)$Pt(CD_3)_3I$ (125 mg, 0.161 mmol) in toluene (15 mL). The reaction was brought out of the box under nitrogen in a glass vessel sealed with a vacuum stopcock and placed in an oil bath (40 °C). The reaction was heated, with stirring, for 24 h. In the air, water (3 mL) was added slowly to the reaction mixture (0 °C). The organic layer (containing the Pt products) was pipetted away from the aqueous layer, and filtered through glass wool. The aqueous layer was washed three times with 5 mL portions of toluene, which were pipetted away and filtered. The filtrate was a clear, colorless solution. A colorless oil remained after the volatiles were removed under vacuum. Recrystallization from $CH_2Cl_2$/pentane afforded colorless needles of ***fac*-1-$d_9$** in 88% yield (94.1 mg). $^1$H NMR ($C_6D_6$): $\delta$ 0.13 (t, w/Pt satellites, 3H, $^2J_{Pt-H} = 43$, $^3J_{P-H} = 6.4$, Pt−C$H_3$), 2.2 (m, 4H, P−C$H_2$–C$H_2$–P), 6.8−7.6 (complex aromatic region). $^{31}$P NMR ($C_6D_6$): $\delta$ 7.4 (s, w/Pt satellites, $^1J_{Pt-P} = 1138$).

**Synthesis, Purification and Characterization of (dppbz)$PtMe_4$ (2).** Under nitrogen, dppbz (0.133 g, 0.297 mmol, dppbz = 1,2-bis-(diphenylphosphino)benzene) and $[PtMe_3I]_4$ (0.133 g, 0.0742 mmol) in THF (10 mL) were allowed to stir overnight. $CH_3Li$ (1.4 M in $Et_2O$, 2.1 mmol) was then added, and the reaction mixture was allowed to stir overnight. The reaction was exposed to air and the excess $CH_3Li$ was quenched by slow addition of water (0.5 mL) to the mixture (0 °C). The volatiles were removed under vacuum. $CH_2Cl_2$ was added to the crude product to dissolve the Pt compounds, leaving behind the inorganic salts. The solution was filtered, and the volatiles were removed from the filtrate under vacuum. This material contained 70% dppbz-$PtMe_4$ (**2**) and 30% dppbz$PtMe_2$ (**7**) ($^{31}$P NMR). Chromatography on neutral alumina (Brockmann II−III) was used to separate **2** from the Pt(II) impurity. **2** was eluted with 3:1 pentane/$CH_2Cl_2$ and the Pt(II) eluted with pure $CH_2Cl_2$. **2** was recrystallized from $CH_2Cl_2$/pentane, and white crystals were isolated in 33% yield (68.7 mg). $^1$H NMR: (THF-$d_8$) $\delta$ −0.51 (t, w/Pt satellites, 6H, $^2J_{Pt-H} = 44$, $^3J_{P-H} = 6.0$, Pt−C$H_3$ trans to methyl), 0.67 (t, w/Pt satellites, 6H, $^2J_{Pt-H} = 60$, $^3J_{P-H} = 7.0$, Pt−C$H_3$ trans to phosphorus), 7.2−7.7 (complex aromatic region); ($C_6D_6$) $\delta$ 0.18 (t, w/Pt satellites, 6H, $^2J_{Pt-H} = 43$, $^3J_{P-H} = 5.9$, Pt−C$H_3$ trans to methyl), 1.44 (t, w/Pt satellites, 6H, $^2J_{Pt-H} = 60$, $^3J_{P-H} = 6.8$, Pt−C$H_3$ trans to phosphorus), 6.8−7.7 (complex aromatic region). $^{13}$C NMR (THF-$d_8$): $\delta$ −2.1 (s, w/Pt satellites, $^1J_{Pt-C} = 400$, Pt-$CH_3$ trans to methyl), 4.0 (dd, w/Pt satellites, $^1J_{Pt-C} = 548$, *trans*-$^2J_{P-C} = 125$, *cis*-$^2J_{P-C} = 4.8$, Pt-$CH_3$ trans to phosphorus), 128.2, 130.3, 131.8, 133.9, 136.1 (aromatic −*C*H), 131.1, 144.6 (aromatic quaternary). $^{31}$P NMR (THF-$d_8$): $\delta$ 15.6 (s, w/Pt satellites, $^1J_{Pt-P} = 1148$). Elemental analysis calculated for $C_{34}H_{36}P_2Pt$: C, 58.20; H, 5.17. Found: C, 58.40; H, 5.23.

**Synthesis and Purification of (dppe)$PtMe_3Et$ (3).** Under nitrogen, EtMgBr (3.0M solution in $Et_2O$, 6.6 mmol) was added to a cooled suspension (−35 °C) of (dppe)$PtMe_3I$ (0.965 g, 1.26 mmol) in toluene (180 mL). The reaction was allowed to stir overnight. The reaction was exposed to air and the excess EtMgBr was quenched by slow addition of water (0.5 mL) to the reaction mixture (0 °C). The volatiles were removed under vacuum. The remaining solid consisted primarily of inorganic salts, (dppe)$PtMe_2$ (**6**) and **3**. The solubility of **6** in $Et_2O$ is significantly less than that of **3**. To achieve crude separation of **3** from the rest of the mixture, the solid residue was treated with ca. 80 mL of $Et_2O$, and the ether solution was transferred to another flask. Evaporation of ether left a residue, which was treated with ca. 50 mL of $Et_2O$ in a similar fashion. Evaporation of the ether provided 0.402 g of solid, of which 77% was **3**. Approximately 51% was ***fac*-3** and 26% was ***mer*-3** ($^{31}$P NMR). Chromatography on alumina was used to separate **3** from Pt(II) impurities. Optimal separation was achieved with neutral alumina (Brockman II−III) and a benzene/pentane solvent system. The Pt(IV) species eluted with 1:1 benzene/pentane and the Pt(II) complexes with pure benzene. While on the column, nearly all of the ***fac*-3** isomerized to ***mer*-3** and formation of (dppe)$PtMe_4$ (**1**) was observed. Later fractions contained progressively more **1**. The fractions with more than 5% **1** were combined and purified with a second column (***mer*-3** elutes before **1**). The final yield of **3** after recrystallization from $CH_2Cl_2$/pentane was 7% (58.8 mg). These samples typically contained 3−5% **1**. *fac*-(dppe)$PtMe_3Et$ (***fac*-3**); $^1$H NMR ($C_6D_6$): $\delta$ 0.14 (t, w/Pt satellites, 3H, $^2J_{Pt-H} = 42$, $^3J_{P-H} = 6.4$, Pt−C$H_3$ trans to ethyl), 0.73 (tq, w/Pt satellites, 2H, $^2J_{Pt-H} = 53$, $^3J_{H-H} = 7.7$, $^3J_{P-H} = 7$, Pt−C$H_2$CH$_3$), 1.16 (t, w/Pt satellites, 3H, $^3J_{Pt-H} = 33$, $^3J_{H-H} = 7.7$, Pt−CH$_2$C$H_3$), 1.51 (t, w/Pt satellites, 6H, $^2J_{Pt-H} = 61$, $^3J_{P-H} = 7.0$, Pt−C$H_3$ cis to ethyl), 2.3 (m, 4H, P−C$H_2$–C$H_2$–P), 7.0−7.4 (complex aromatic region). $^{13}$C NMR ($C_6D_6$): $\delta$ −4.5 (s, w/Pt satellites, $^1J_{Pt-C} = 380$, Pt-$CH_3$ trans to ethyl), −2.8 (s, w/Pt satellites, $^1J_{Pt-C} = 396$, Pt-$CH_2$CH$_3$), 3.4 (dd, w/Pt satellites, $^1J_{Pt-C} = 567$, *trans*-$^2J_{P-C} = 122$, *cis*-$^2J_{P-C} = 6.4$, Pt-$CH_3$ cis to ethyl), 13.1 (s (br), Pt−$CH_2$CH$_3$), 27.4 (complex pattern, P-$CH_2$–$CH_2$–P), 128−133 (aromatic signals, unresolved). $^{31}$P NMR ($C_6D_6$): $\delta$ 5.2 (s, w/Pt satellites, $^1J_{Pt-P} = 1147$). *mer*-(dppe)$PtMe_3Et$ (***mer*-3**); $^1$H NMR ($C_6D_6$): $\delta$ 0.12 (t, w/Pt satellites, 6H, $^2J_{Pt-H} = 44$, $^3J_{P-H} = 6.4$, Pt−C$H_3$ trans to methyl), 1.52 (t, w/Pt satellites, 3H, $^2J_{Pt-H} = 61$, $^3J_{P-H} = 7.0$, Pt−C$H_3$ trans to phosphorus), 1.58 (dt, w/Pt satellites, 3H, $^3J_{Pt-H} = 54$, $^4J_{P-H} = 11.6$, $^3J_{H-H} = 7.7$, Pt−CH$_2$C$H_3$), 2.2 (m, 4H, P−C$H_2$–C$H_2$–P), 2.32 (tq, w/Pt satellites, 2H, $^2J_{Pt-H} = 69$, $^3J_{P-H} = 8$, $^3J_{H-H} = 7.7$, Pt−C$H_2$CH$_3$), 7.0−

7.4 (complex aromatic region). $^{13}$C NMR ($C_6D_6$): $\delta$ −3.8 (s, w/Pt satellites, $^1J_{Pt-C}$ = 416, Pt-*C*H$_3$ trans to methyl), 3.2 (dd, w/Pt satellites, $^1J_{Pt-C}$ = 573, *trans*-$^2J_{P-C}$ = 124, *cis*-$^2J_{P-C}$ = 5.5, Pt-*C*H$_3$ trans to phosphorus), 9.7 (dd, w/Pt satellites, $^1J_{Pt-C}$ = 547, *trans*-$^2J_{P-C}$ = 124, *cis*-$^2J_{P-C}$ = 4.7, Pt-*C*H$_2$CH$_3$), 15.1 (s (br), Pt−CH$_2$*C*H$_3$), 28.5 (complex pattern, P-*C*H$_2$–*C*H$_2$–P), 128−133 (aromatic signals, unresolved). $^{31}$P NMR ($C_6D_6$): $\delta$ 6.4 (d, w/Pt satellites, $^1J_{Pt-P}$ = 1141, $^2J_{P-P}$ = 8.8, phosphorus trans to methyl), 7.4 (d, w/Pt satellites, $^1J_{Pt-P}$ = 992, $^2J_{P-P}$ = 8.8, phosphorus trans to ethyl).

**Synthesis, Purification and Characterization of *fac*-(dppe)-PtMe$_3$H (4).** Under nitrogen, NaCNBH$_3$ (99.4 mg, 1.58 mmol) was added to a solution of *fac*-(dppe)PtMe$_3$(OAc) (356 mg, 0.511 mmol) in THF (10 mL). The reaction was allowed to stir for 15 min, and then the volatiles were removed under vacuum. A colorless oil remained. Et$_2$O (10 mL) was added to the oil and then removed under vacuum (repeated three times) to leave a slightly off-white solid remained. Under nitrogen, some of the crude product was removed for analysis by $^{31}$P NMR, which showed 75% **4** and 25% (dppe)PtMe$_2$ (**6**). The crude product was rinsed with Et$_2$O (25 mL total), and the solution was filtered through a pipet packed with glass wool, followed by removal of the volatiles under vacuum. Recrystallization from Et$_2$O/pentane gave colorless crystals. The first crop contained few crystals, but the material was pure **4** by NMR. A second recrystallization afforded significantly more material, but the crystals contained 79% **4** and 21% **6** ($^{31}$P NMR). Of the solid isolated in the second crop (178 mg), only 79% was **4** (141 mg), which is 43% of the theoretical yield. $^1$H NMR ($C_6D_6$): $\delta$ −8.6 (br t w/Pt satellites, 1H, $^1J_{Pt-H}$ = 706, $^2J_{P-H}$ = 12.9, Pt-*H*), −0.14 (dt, w/Pt satellites, 3H, $^2J_{Pt-H}$ = 43, $^3J_{P-H}$ = 6.4, $^3J_{H-H}$ = 2.8, Pt−C*H*$_3$ trans to hydride), 1.45 (dt, w/Pt satellites, 6H, $^2J_{Pt-H}$ = 60, $^3J_{P-H}$ = 7.1, $^3J_{H-H}$ = 1.3, Pt−C*H*$_3$ trans to phosphorus), 1.8, 2.3 (m. 4H, P−*C*H$_2$–*C*H$_2$–P), 7.0−7.4 (complex aromatic region). $^{13}$C NMR (THF-$d_8$): $\delta$ −8.5(d, w/Pt satellites, $^1J_{Pt-C}$ = 516. $^1J_{H-C}$ = 117, Pt-*C*H$_3$ trans to hydride), −1.1 (d, w/Pt satellites, $^1J_{Pt-C}$ = 610, *trans*-$^2J_{P-C}$ = 98, *cis*-$^2J_{P-C}$ = 5.5, Pt-*C*H$_3$ trans to phosphorus), 27 (complex pattern, P-*C*H$_2$–*C*H$_2$–P), 127−133 (aromatic signals, unresolved). $^{31}$P NMR: ($C_6D_6$) $\delta$ 24.3 (s, w/Pt satellites, $^1J_{Pt-P}$ = 1218); (THF-$d_8$) $\delta$ 24.4 (s, w/Pt satellites, $^1J_{Pt-P}$ = 1232).

**Synthesis, Purification and Characterization of *fac*-(dppe)-PtMe$_3$D (4-$d_1$).** Under nitrogen, NaBD$_4$ (21.6 mg, 0.516 mmol) was added to a solution of *fac*-(dppe)PtMe$_3$(OAc) (71.9 mg, 0.103 mmol) in THF (15 mL). The reaction was allowed to stir for 15 min, then filtered through a pipet packed with glass wool. The volatiles were removed under vacuum. The resulting yellow oil was dissolved in Et$_2$O (5 mL), which was removed under vacuum. This was repeated three times, and yellow solid remained. Recrystallization from Et$_2$O/pentane yielded a pale yellow powder (45.4 mg), which contained 80% **4-$d_1$** and 20% (dppe)PtMe$_2$ (**6**) ($^{31}$P NMR). The amount of **4-$d_1$** in the powder was calculated to 55% (36.3 mg) of the theoretical yield. $^1$H NMR ($C_6D_6$): $\delta$ −0.14 (t, w/Pt satellites, 3H, $^2J_{Pt-H}$ = 43, $^3J_{P-H}$ = 6.3, Pt−C*H*$_3$ trans to deuteride), 1.46 (t, w/Pt satellites, 6H, $^2J_{Pt-H}$ = 60, $^3J_{P-H}$ = 7.0, Pt−C*H*$_3$ trans to phosphorus), 1.7, 2.3 (m. 4H, P−C*H*$_2$–C*H*$_2$–P), 6.9−7.4 (complex aromatic region). $^{31}$P NMR ($C_6D_6$): $\delta$ 24.4 (s, w/Pt satellites, $^1J_{Pt-P}$ = 1219).

**Synthesis, Purification, and Characterization of *fac*-(dppbz)-PtMe$_3$H (5).** Under nitrogen, a THF solution of BH$_3$·THF (0.120 mL, 0.120 mmol) was added to a solution of *fac*-(dppbz)PtMe$_3$(OAc) (87.7 mg, 0.118 mmol) in THF (10 mL). The reaction was allowed to stir for 30 min, and then the volatiles were removed under vacuum and the resulting pale yellow solid was left under vacuum overnight. Under nitrogen, the solid was rinsed with toluene (30 mL), which yielded a colorless solution and insoluble yellow solid. The solution was filtered through a pipet packed with glass wool and a plug of diatomaceous earth. The volatiles were removed under vacuum, and the resulting white solid was recrystallized from THF/pentane. White crystals were isolated (55.3 mg), which contained 91% **5** and 9% (dppbz)PtMe$_2$ (**7**) ($^{31}$P NMR). The amount of **5** in this mixture was calculated to be 62% (50.3 mg) of the theoretical yield. $^1$H NMR ($C_6D_6$): $\delta$ −8.3 (t (br), w/Pt satellites, 1H, $^1J_{Pt-H}$ = 689, $^2J_{P-H}$ = 13.2, Pt-*H*), −0.27 (dt, w/Pt satellites, 3H, $^2J_{Pt-H}$ = 45, $^3J_{P-H}$ = 6.4, $^3J_{H-H}$ = 2.9, Pt−C*H*$_3$ trans to hydride), 1.50 (dt, w/Pt satellites, 6H, $^2J_{Pt-H}$ = 60, $^3J_{P-H}$ = 7.1, $^3J_{H-H}$ = 1.1, Pt−C*H*$_3$ trans to phosphorus), 6.7−7.8 (complex aromatic region). $^{13}$C NMR (THF-$d_8$): $\delta$ −9.5 (d, w/Pt satellites, $^1J_{Pt-C}$ = 517, $^2J_{H-C}$ = 116, Pt-*C*H$_3$ trans to hydride), 3.7 (d, w/Pt satellites, $^1J_{Pt-C}$ = 618, $^2J_{P-C}$ = 99, Pt-*C*H$_3$ trans to phosphorus), 129−137 (aromatic signals, unresolved. $^{31}$P NMR ($C_6D_6$): $\delta$ 24.7 (s, w/Pt satellites, $^1J_{Pt-P}$ = 1218).

**Synthesis, Purification and Characterization of *fac*-(dppbz)-PtMe$_3$D (5-$d_1$).** Under nitrogen, NaBD$_4$ (17.3 mg, 0.413 mmol) was added to a solution of (dppbz)PtMe$_3$(OAc) (54.1 mg, 0.0725 mmol) in THF (10 mL). The reaction was allowed to stir for 1 h, and then the volatiles were removed under vacuum. The resulting white solid was left under vacuum overnight. Under nitrogen, the solid was rinsed with toluene (20 mL), and the solution was filtered through a pipet packed with glass wool and a plug of diatomaceous earth. The volatiles were removed under vacuum and the resulting solid was recrystallized from THF/pentane. White crystalline solid was isolated (28.9 mg), which contained 85% **5-$d_1$** and 15% (dppbz)PtMe$_2$ (**7**). The amount of **5-$d_1$** in the crystals was calculated to be 49% (24.6 mg). $^1$H NMR ($C_6D_6$): $\delta$ −0.27 (t, w/Pt satellites, 3H, $^2J_{Pt-H}$ = 45, $^3J_{P-H}$ = 6.4, Pt−C*H*$_3$ trans to deuteride), 1.50 (t, w/Pt satellites, 6H, $^2J_{Pt-H}$ = 60, $^3J_{P-H}$ = 7.1, Pt−C*H*$_3$ trans to phosphorus), 6.7−7.8 (complex aromatic region). $^{31}$P NMR ($C_6D_6$): $\delta$ 24.7 (s, w/Pt satellites, $^1J_{Pt-P}$ = 1218).

**Synthesis and Purification of (dppe)PtMe$_2$ (6).** An alternative preparation to that previously reported for **6** was used.[31] Under nitrogen, an ether solution of CH$_3$Li (32 mL, 45 mmol) was slowly added with stirring to a cooled suspension (−35 °C) of (dppe)PtCl$_2$ (5.840 g, 8.789 mmol) in toluene (80 mL). The reaction was allowed to come to ambient temperature, and after stirring overnight, the solution was yellow and cloudy. In the air, water (2 mL) was added dropwise to the reaction mixture (0 °C). The volatiles were removed under vacuum and hot toluene (180 mL) was added to the flask to separate the organometallic product from the inorganic salts. The mixture was filtered through pipets packed with glass wool, and the volatiles were removed from the filtrate, which left behind a yellow solid. The solid was dissolved in CH$_2$Cl$_2$ (150 mL), and the solution was filtered through a small plug of alumina. The filtrate was concentrated with gentle heat (45 mL), and the solution was place in the freezer (−20 °C). Colorless crystals were isolated and washed with cold CH$_2$Cl$_2$ and pentane. After drying under vacuum, the yield was 89% (4.869 g).

**Synthesis and Characterization of (dppe)PtMeEt (8).** Under nitrogen, an ether solution of EtMgBr (0.2 mL, 0.6 mmol) was slowly added with stirring to (dppe)PtMeCl (70.6 mg, 0.110 mmol) in toluene (10 mL). The reaction was allowed to stir overnight, after which time the solution was cloudy. In the air, water (0.2 mL) was added dropwise to the reaction mixture (0 °C). The volatiles were removed under vacuum and toluene (20 mL) was added to the flask to separate the organometallic product from the inorganic salts. The mixture was filtered through pipets packed with glass wool, and the volatiles were removed from the filtrate, which left behind an off-white solid. Recrystallization from CH$_2$Cl$_2$/pentane at −24 °C produced colorless crystalline needles, 30.7 mg (44% yield). $^1$H NMR ($C_6D_6$): $\delta$ 1.57 (t, w/Pt satellites, 3H, $^2J_{Pt-H}$ = 72, $^3J_{P-H}$ = 7.4, Pt−C*H*$_3$), 1.74 (dt, w/Pt satellites, 3H, $^3J_{Pt-H}$ = 70, $^3J_{H-H}$ = 8.7, $^4J_{P-H}$ = 7.7, Pt−CH$_2$*C*H$_3$), 1.85 (m, 4H, P−C*H*$_2$–C*H*$_2$–P), 2.31 (tq, w/Pt satellites, 2H, $^2J_{Pt-H}$ = 75, $^3J_{H-H}$ = 8.7, $^3J_{P-H}$ = 7.7, Pt−C*H*$_2$CH$_3$), 7.0−7.4 (complex aromatic region). $^{31}$P NMR ($C_6D_6$): $\delta$ 48.6 (d, w/Pt satellites, $^1J_{Pt-P}$ = 1850, $^2J_{P-P}$ = 7.3, phosphorus trans to methyl), 45.0 (d, w/Pt satellites,$^1J_{Pt-P}$ = 1536, $^2J_{P-P}$ = 7.3, phosphorus trans to ethyl). Elemental analysis calculated for C$_{29}$H$_{32}$P$_2$Pt: C, 54.62; H, 5.05. Found: C, 54.51; H, 4.97.

**Crystal Structure Determination.** Colorless cubes of (dppe)PtMe$_4$ (**1**) were obtained from a solution of **1** in CH$_2$Cl$_2$ that was layered with pentane, then cooled to −20 °C. The crystals were rinsed with

pentane and excess solvent was removed under vacuum. The same procedure was used to obtain colorless plates of (dppbz)$PtMe_4$ (**2**). Colorless plates of *fac*-(dppe)$PtMe_3H$ (**4**) were obtained under a nitrogen atmosphere from a solution of **4** in $Et_2O$ that was layered with pentane and cooled to −35 °C. The crystals were rinsed with pentane and excess solvent was removed under vacuum.

Crystallographic data for **1** and **2** were collected at the University of Washington X-ray crystallography lab, using a Nonius Kappa CCD with Mo Kα radiation. The crystals of **1** and **2** were mounted on a glass capillary with epoxy. Non-hydrogen atoms were refined anisotropically by full-matrix least-squares. Hydrogen atoms were placed with idealized geometry and refined using a riding model. All intensities were integrated and subsequently scaled with the Denzo-SMN package.[53]

Crystallographic data for **4** were also collected at the University of Washington X-ray crystallography lab, using a Nonius Kappa CCD with Mo Kα radiation. The crystals of **4** were mounted on a glass capillary under oil. Non-hydrogen atoms were refined anisotropically by full-matrix least-squares. All hydrogen atoms were located from difference maps except for H(1C) on $C_1$ (methyl hydrogen), which was placed. Hydrogen atoms were refined with a riding model except for the hydride, H(1Pt), which was refined isotropically. All intensities were integrated and subsequently scaled with the Denzo-SMN package.[53] The crystallographic data for complexes **1**, **2**, and **4** can be found in Table 1. Selected bond lengths and angles appear in Tables 2 and 3.

**Kinetics Experiments for 1, 2, and 3.** In a typical kinetics experiment, the desired compound was weighed to microgram accuracy (typically 3−10 mg), and transferred to a sealable medium-walled NMR tube. The tube was evacuated and deuterated solvent was vacuum transferred into the tube. An internal standard, either dioxane or hexamethyldisiloxane (ca. 4 Torr), was added via a known volume bulb (16.95 mL, 0.004 mmol). The tube was flame sealed under vacuum. After warming to room temperature, the volume of the solution was measured (ca. 0.30 mL). An initial $^1$H NMR spectrum was collected. The tube was heated in an oil bath at the desired temperature for a specified amount of time, then quickly cooled in an ice bath. Three $^1$H NMR spectra were acquired after each heating period, and the integrals were averaged. The reaction was followed by monitoring the disappearance of the axial methyl signal relative to the dioxane ($T_1$ = 17 s, pulses space 90 s apart) or hexamethyldisiloxane ($T_1$ = 8 s, pulses spaced 40 s apart) standard. The tube was frozen at −20 °C when not in the oil bath or spectrometer. Kinetics samples were followed for at least three half-lives (ca. 10 points) and a rate constant was obtained by a least squares linear regression method.

**Crossover Study. 1** (6.849 mg, 0.01048 mmol) and **1-*d*$_{12}$** (6.981 mg, 0.01049 mmol) were dissolved in acetone (1.00 mL). An aliquot (0.67 mL) was transferred to a pressure/vacuum valve NMR tube, and the solvent was removed under vacuum. $C_6D_6$ (0.3 mL) was vacuum transferred into the tube, which was then sealed by closing the valve. An initial $^{31}$P NMR spectrum was collected, which showed only **1** and **1-*d*$_{12}$**. The tube was heated in an oil bath at 165 °C for 50 h. The $^{31}$P NMR spectrum showed **1**, **1-*d*$_{12}$**, **6** ($\delta$ 47.35, $^1J_{Pt-P}$ = 1779), **6-*d*$_6$** ($\delta$ 47.49, $^1J_{Pt-P}$ = 1769), and what has been assigned as **6-*d*$_3$** ($\delta$ 47.42, $^1J_{Pt-P}$ = 1774). Unfortunately, even at high field (202.5 MHz), baseline resolution of the Pt(II) products was not observed. In the $^1$H NMR (500 MHz) spectrum, a sharp signal for $CH_3CH_3$ ($\delta$ 0.80) was observed. No other signals which could be assigned to $CH_3CD_3$ were detected. The gases produced in the thermolysis were analyzed directly by high-resolution mass spectrometry. The spectrum was compared to the high-resolution mass spectra of $CH_3CH_3$, $CH_3CD_3$, and $CD_3CD_3$. The mass spectra of the authentic samples provided information about the relative intensities of the fragments. The base peak (highest intensity) was $C_2H_4$ for ethane, $C_2H_2D_2$ for ethane-$d_3$ and $C_2D_4$ for ethane-$d_6$. In the analysis of the gaseous products from the thermolysis of **1** and **1-*d*$_{12}$**, the intensity of the base peak for each isotopomer of ethane was calculated. These values were used to represent the amount of each isotopomer present in the mixture. This analysis showed that less than 4% of gas mixture was $CH_3CD_3$, with approximately 43% $CH_3CH_3$ and 53% $CD_3CD_3$.

**Thermolysis of 6 and 6-*d*$_6$ in $C_6D_6$.** An NMR tube was loaded with **6** (6.002 mg, $9.625 \times 10^{-3}$ mmol) and **6-*d*$_6$** (6.098 mg, $9.685 \times 10^{-3}$ mmol). $C_6D_6$ (0.35 mL) was vacuum transferred into the tube and the tube was flame-sealed. The initial $^{31}$P NMR spectrum showed only **6** and **6-*d*$_6$**. The tube was then heated in an oil bath at 165 °C for 12 h. After heating, the $^{31}$P NMR spectrum showed **6** ($\delta$ 47.35, $^1J_{Pt-P}$ = 1779), **6-*d*$_6$** ($\delta$ 47.49, $^1J_{Pt-P}$ = 1769) and a significant amount of **6-*d*$_3$** ($\delta$ 47.42, $^1J_{Pt-P}$ = 1774).[34]

**GC/MS Analysis of (dppe)$PtMe_3$Et (3) Thermolysis Products.** A bomb was charged with **3** (52.8 mg, 0.0791 mmol) and benzene (20 mL). After three freeze−pump−thaw cycles, the solution was heated for 12 h at 165 °C. The solution was cooled to −78 °C and the volatiles were transferred under static vacuum to a bomb with a septum sideport, cooled to −196 °C. The volatiles were sampled with a Gastight syringe and injected into the GC/MS. The methane appeared immediately, and was overlapping with a large air peak. This was followed by ethane, then ethylene and finally propane. The gases were identified by their unique mass spectral peaks.

**Calibration for GC/FID Analysis.** Using a known volume bulb (16.95 mL), equal pressures of ethane, ethylene and propane (ca. 170 Torr, 0.15 mmol) were transferred to a bomb with a septum sideport, cooled to −196 °C. This mixture was sampled with a Gastight syringe equipped with a locking valve, and then injected into the GC/FID. The three peaks were integrated and the data from two separate runs was compared. The signals for ethane and ethylene were found to be lower than expected, and correction factors were calculated. Ethane intensities needed to be multiplied by 1.014, and ethylene intensities needed to be multiplied by 1.032.

**GC/FID Analysis of (dppe)$PtMe_3$Et (3) Thermolysis Products.** Under nitrogen, a bomb was charged with **3** (20.854 mg, 0.031 234 mmol), ferrocene (4.459 mg, 0.02397 mmol) and $C_6D_6$ (2 mL). An aliquot (0.3 mL) was removed, and transferred to an NMR tube. Initial $^1$H and $^{31}$P NMR spectra were collected, and the only signals corresponded to **3** and a small amount of (dppe)$PtMe_4$ (**1**, ca. 5%). The bomb was heated 12 h at 165 °C, then frozen at −78 °C. Under static vacuum, the volatiles were transferred to bomb with a septum sideport. The volatiles were condensed in the septum bomb at −196 °C (liquid nitrogen). The reaction mixture was warmed to room temperature, and the transfer process was repeated two more times. The gaseous products of the thermolysis were then sampled with a gastight syringe equipped with a locking valve and injected into the GC/FID. Peaks for methane (3.7 min), ethane (4.0 min), ethylene (4.5 min) and propane (6.4 min) were detected and integrated. The injections were repeated until the signal/noise was too poor to continue. The relative amounts of ethylene, ethane and propane were then calculated using the correction factors from the calibration (see above). The ratio of ethylene to propane to ethane was 75:18:7. The numbers for methane were not an accurate representation of the methane produced in the reaction, because methane does not completely condense at −196 °C, so not all of it was collected in the septum bomb. Finally, a small aliquot (0.3 mL) of the post-thermolysis reaction mixture was transferred to an NMR tube and analyzed by $^1$H and $^{31}$P NMR, which showed mostly (dppe)$PtMe_2$ (**6**, 91% from integration of $^1$H NMR) and a small amount of (dppe)PtMeEt (**8**, 4% from integration of $^1$H NMR).

**Kinetics Experiments for 4 and 5.** In a typical kinetics experiment, the desired compound was weighed (3−5 mg), under nitrogen, to the nearest tenth of a milligram. The compound was then transferred into a sealable NMR tube. The tube was evacuated and deuterated solvent was vacuum transferred into the tube. Dioxane (ca. 3 Torr) was added via a known volume bulb (16.95 mL, $3 \times 10^{-3}$ mmol) as an internal standard. The tube was flame sealed under vacuum or under a partial pressure of nitrogen (ca. 500 Torr). After warming to room temperature,

(53) Otinowski, Z.; Minor, W. *Methods Enymol.* **1996**, *276*, 307.

the volume of the solution (ca. 0.30 mL) was measured. An initial $^1$H NMR spectrum was collected. Two methods were employed for monitoring the thermolysis reaction. NMR tubes sealed under vacuum were heated in an oil bath at the desired temperature for a specified amount of time, then quickly cooled in an ice bath. Three $^1$H NMR spectra were acquired after each heating period, and the integrals were averaged. The reaction was followed by disappearance of the axial methyl signal of *fac*-$L_2PtMe_3H$ relative to the dioxane standard ($T_1$ = 17 s, pulses spaced 90 s apart). The tube was frozen at −20 °C when not in the oil bath or spectrometer. Several kinetics samples were heated in the NMR probe (AM 500 or DRX 499). Due to solvent reflux when sealed under vacuum, these NMR tubes were sealed under a partial pressure of nitrogen. The spectrometer was programmed to collect a specified number of spectra, each spectrum separated by a specified amount of time, which was at least 90 s to allow for full relaxation of the dioxane standard. The progress of the reaction was monitored by integrating the axial methyl signal against the dioxane standard. In both cases, kinetics samples were followed for three half-lives (ca. 10 points) and a rate constant was obtained by a least squares linear regression method. The identity of the products was confirmed by comparison to NMR spectra of authentic samples.

**Acknowledgment.** This work was supported by the National Science Foundation. The X-ray structure determinations were performed by Dr S. Lovell and Dr. W. Kaminsky (UW).

**Supporting Information Available:** Kinetics plots for the thermolyses of **1**, **4**, **4-*d*$_1$**, **5,** and **5-*d*$_1$** and kinetics plots for the isomerizations of complexes ***fac*-1-*d*$_9$** and ***fac*-3** (PDF); X-ray crystallographic data files for complexes **1**, **2**, and **4** (CIF). This material is available free of charge via the Internet at http://pubs.acs.org.

JA029140U